Cerebral Cortex, October 2015;25: 4009–4028

doi: 10.1093/cercor/bhu290
Advance Access Publication Date: 5 December 2014
Original Article

ORIGINAL ARTICLE

Increased Visual Stimulation Systematically Decreases Activity in Lateral Intermediate Cortex

Shahin Nasr[1,2], Heiko Stemmann[3], Wim Vanduffel[1,2,3], and Roger B. H. Tootell[1,2]

[1]Athinoula A. Martinos Center for Biomedical Imaging, Massachusetts General Hospital, Charlestown, MA 02129, USA, [2]Department of Radiology, Harvard Medical School, Charlestown, MA 02129, USA, and [3]Laboratory of Neuro and Psychophysiology, KU Leuven Medical School, 3000 Leuven, Belgium

Address correspondence to Shahin Nasr. Email: shahin@nmr.mgh.harvard.edu

Abstract

Previous studies have attributed multiple diverse roles to the posterior superior temporal cortex (STC), both visually driven and cognitive, including part of the default mode network (DMN). Here, we demonstrate a unifying property across this multimodal region. Specifically, the lateral intermediate (LIM) portion of STC showed an unexpected feature: a progressively decreasing fMRI response to increases in visual stimulus size (or number). Such responses are reversed in sign, relative to well-known responses in classic occipital temporal visual cortex. In LIM, this "reversed" size function was present across multiple object categories and retinotopic eccentricities. Moreover, we found a significant interaction between the LIM size function and the distribution of subjects' attention. These findings suggest that LIM serves as a part of the DMN. Further analysis of functional connectivity, plus a meta-analysis of previous fMRI results, suggests that LIM is a heterogeneous area including different subdivisions. Surprisingly, analogous fMRI tests in macaque monkeys did not reveal a clear homolog of LIM. This interspecies discrepancy supports the idea that self-referential thinking and theory of mind are more prominent in humans, compared with monkeys.

Key words: DMN, fMRI, homology, size response function, temporal cortex

Introduction

In most animals, extensive neural processing is devoted to sensory perception of physical variations in the external world. However, in humans (and perhaps other species), the "internal world" also strongly influences sensory perception and its underlying the neural processes. These internal representations include: self-referential and affective decision-making (Gusnard et al. 2001; Wicker et al. 2003; D'Argembeau et al. 2005, 2010; van der Meer et al. 2010; Qin and Northoff 2011; Denny et al. 2012; Molnar-Szakacs and Uddin 2013), thinking about the future (Schacter and Addis 2007; Arzy et al. 2008; Andrews-Hanna et al. 2010; Spreng and Grady 2010) and instances involving theory of mind (ToM)(Gallagher and Frith 2003; Saxe et al. 2004; Ochsner et al. 2004; Spreng et al. 2009).

One striking manifestation of such internal representations is the default mode network (DMN). The DMN is a set of cortical areas that show higher fMRI activity during specific internal processing states (Shulman et al. 1997; Mazoyer et al. 2001; Raichle et al. 2001; Buckner et al. 2008; Andrews-Hanna et al. 2010). Two areas comprise the core (i.e., the main "hub") of the DMN: the medial prefrontal cortex (mPFC) and the posterior cingulate cortex (PCC). These core areas are functionally connected with additional subareas of the DMN including the inferior parietal lobe (IPL), angular gyrus (ANG), temporal-parietal junction (TPJ),

lateral temporal cortex (LTC), and the temporal pole (Greicius et al. 2003; Buckner et al. 2008; Hagmann et al. 2008; Andrews-Hanna et al. 2010; Mantini and Vanduffel 2013). Many studies have focused on the role of the DMN core areas (i.e., mPFC and PCC) in "stimulus-independent" and "task-unrelated" thinking (McKiernan et al. 2006; Mason et al. 2007), including social cognitive processing, retrieval of autobiographical memory, and self-referential decision-making (for review, see Buckner et al. 2008; Mantini and Vanduffel 2013; Molnar-Szakacs and Uddin 2013).

In comparison with these studies of the DMN core areas, the role of DMN subareas remains less understood. Here, we mainly focus on 1 of those subareas, the LTC, which is located near the anterior-lateral border of classic visual cortex along the superior temporal sulcus (STS). The specific location of LTC varies somewhat across different studies, including parts of the IPL, the ANG, and the superior/middle temporal gyri (Buckner et al. 2008; Andrews-Hanna et al. 2010; Mantini and Vanduffel 2013).

Activity in LTC has also been interpreted somewhat differently across studies. Some studies suggest that the more posterior portion of LTC (including angular and superior temporal gyrus) is involved in processing ToM (Saxe and Kanwisher 2003; Young et al. 2007; Van Overwalle and Baetens 2009; Dodell-Feder et al. 2011; Heatherton 2011; Sebastian et al. 2011). Other studies highlight the role of LTC in autobiographic memory and internal representations of the self (Buckner et al. 2008; Andrews-Hanna et al. 2010; Spreng and Grady 2010; Denny et al. 2012; Bado et al. 2013).

In the sensory realm, additional studies have reported that nearby or overlapping cortical regions (including the medial temporal gyrus and the STS) are activated during face processing, especially during the encoding of eye gaze direction (Puce et al. 1998; Pelphrey et al. 2005; Engell and Haxby 2007; Ethofer et al. 2011) and facial expression (Haxby et al. 2000; Winston et al. 2004; Engell and Haxby 2007; Said et al. 2011), and also the visual interpretation of biological motion (Puce et al. 1996; Beauchamp et al. 2003; Thompson et al. 2007; Fox et al. 2009; Jastorff and Orban 2009; Pinsk et al. 2009; Furl et al. 2011; Julian et al. 2012; Avidan et al. 2014). Presumably, all these processes involve interpretations of actions in other people, based on comparison with internal representations of analogous experiences in the observer.

Based on this evidence, and because LTC is located near relatively well-studied regions of visual cortex, 1 hypothesis is that LTC is involved in the transition of information from external (e.g., sensory) to internal representation(s). Here, we used fMRI to study that functional transition, based on graded sensory manipulations that we found to systematically influence these internal representations.

More specifically, it is known that fMRI activity decreases significantly in the DMN when subjects direct their attention toward more salient (i.e., more "immediate") stimuli in the surrounding environment, compared with passive viewing of a spatially uniform screen and/or mentation tasks (Shulman et al. 1997; Raichle et al. 2001; Greicius and Menon 2004; Buckner et al. 2008).

Importantly, such decreased fMRI activity to increased visual stimulation in the DMN is opposite in sign to that typically found when measuring visually driven fMRI responses throughout primate visual cortex. From early retinotopic areas to high-level category-selective areas, presentation of a wide range of visual stimuli increases the level of fMRI activity relative to that found during fixation on a uniform gray screen (i.e., a common baseline condition in visual system studies). Moreover, in visual cortex, this visually driven activity increases when the (retinal) stimulus size is made larger in the visual field (Ito et al. 1995; Allison et al. 1999; Ashbridge et al. 2000; Op de Beeck and Vogels 2000; Konkle and Oliva 2012). Thus, 1 corollary of our current hypothesis is that the sign of the response to increased visual stimulation will reverse in the cortical map, at or near the border between classic visual cortex and the nearby DMN subarea, LTC. If so, this would furnish a clear-cut opportunity to study where and how the sensory and internal processing systems are functionally interconnected, and how they interact with each other, at the level of fMRI.

We addressed these questions in 7 experiments. In Experiment 1, we systematically tested for a paradoxically decreased response to increased stimulus size in the vicinity of LTC, and (as a control) throughout the brain. These results confirmed our hypothesis, which enabled the subsequent experiments. We refer to the region that showed decreased responses to larger stimuli as the lateral intermediate ("LIM") region. Experiment 2 compared the effect of object "size" versus object "number" on the evoked activity in LIM, to distinguish between the effects of object size per se versus a more general increase in the surface area of the stimulated visual field. Experiment 3 tested whether the distinctive LIM responses depend on stimulus eccentricity, which is 1 axis of visual field position. Experiment 4 began relating these sensory (externally driven) findings to the cognitive (internal) realm, by systematically varying the distribution of spatial attention and testing its influence on activity within LIM. Because previous experiments have reported additional functional properties (including biological motion- and face-selective responses) in the vicinity of LIM, Experiment 5 tested the overlap between LIM and these other functions, in additional experiments and in a meta-analysis of previous data. To clarify the underlying neural circuits, Experiment 6 mapped the distinct functional connectivity within LIM, relative to the rest of the brain.

The confluence of internal and externally driven influences found in this general region of human cortex (Experiments 1–6) raised a question: Do analogous cortical regions exist in other primates such as the macaque monkey? This question has significant implications. Many studies have shown that the organization of visual cortex (representing the external world) is largely conserved across these 2 species (Van Essen et al. 2001; Tootell et al. 2003; Orban et al. 2004). However, the presumptive homolog of DMN (representing the internal world) is much less studied in nonhuman primates (but see Rilling et al. 2007; Vincent et al. 2007; Kojima et al. 2009; Mantini et al. 2011; Mars et al. 2013). Multiple lines of evidence suggest that this region of occipitoparietal cortex is proportionately smaller in macaques compared with humans (Orban et al. 2004; Sereno and Tootell 2005). Thus, an LIM homolog may be either absent or significantly smaller in macaque monkeys, compared with LIM in humans. Alternatively, it may be that LIM is also prominent and extensive in macaque, to the extent that LIM serves a crucial function common to both species. To clarify this issue, Experiment 7 used analogous fMRI techniques to test for an LIM homolog in awake fixating macaque monkeys.

Methods

Human Experiments

Subjects

For each experiment, human subjects were selected randomly from a pool of 24 subjects (13 females), aged 20–36 years. All subjects had normal or corrected-to-normal visual acuity and radiologically normal brains, without history of neuropsychological disorder. All experimental procedures conformed to NIH guidelines and were approved by Massachusetts General Hospital protocols. Written informed consent was obtained from all subjects.

Stimuli. *Experiment 1A*. This experiment included images from 3 different image categories including faces (20 images), nonface everyday objects (40 images), and irregular shapes (20 images) (Fig. 1A). In all experiments, images were adjusted for achromatic contrast, based on root mean square. In each scan session, trials were blocked according to the stimulus category (faces vs. nonface everyday objects vs. irregular shapes) and size (i.e., small [0.35 degrees^2] vs. large [73.50 degrees^2]). In this and the following experiments, 16 images were presented in each block. Image duration was 1 s.

Experiment 1B. Thirty different images of face and nonface everyday objects (independent of those used in Experiment 1A) were presented randomly in each block. Stimuli were blocked according to their retinal size (area), varying from 0° (i.e., a uniform gray screen, used as a baseline condition) through 0.04 degrees^2, 0.34 degrees^2, 11.40 degrees^2, and 181.66 degrees^2. Other details are similar to those in Experiment 1.

Experiment 2. This experiment used 19 different images of face and nonface everyday objects, independent of those used in Experiments 1A and 1B. In those blocks in which multiple objects were presented, 1 object was always positioned at the center of screen, and 9 other objects were positioned at random locations surrounding it on the display screen, without any overlap between objects. Stimuli were images of face and nonface objects with the following configurations: 1) a single small object (0.51 degrees^2 visual field area), 2) a single medium object (5.59 degrees^2), 3) a single large object (55.95 degrees^2) and 4) 10 medium-sized objects presented concurrently (summed visual field area = 55.95 degrees^2) (Fig. 2A). Importantly, the total visual field area subtended by all stimuli was equivalent in the latter 2 conditions (i.e., a large single face/object vs. 10 medium-sized faces/objects; both 55.95 degrees^2).

Experiment 3. Thirty different images of face and nonface everyday objects were presented, which were independent of those used in Experiments 1 and 2. Stimulus size (0.31 vs. 70.50 degrees^2), eccentricity (10° vs. 15° vs. 20°), and laterality (left vs. right) were systematically varied between blocks. To maximize the visual field extent (24.8°), the fixation point was positioned near either the left (50% of runs) or the right edges of the screen within a given run, and it remained at the same location throughout each block. At the beginning of each run, the subject had sufficient time to locate and fixate the fixation point; then the scanning started.

Experiment 4A. Twenty different images of face and nonface everyday objects were presented randomly within each experiment block. Stimuli size varied across the blocks (i.e., small vs. large; 0.34 degrees^2 vs. 184.29 degrees^2, respectively).

Experiment 4B. The stimulus was a radial checkerboard (127.60 degrees^2) in which each check reversed in contrast every 1 s (i.e., 0.5 Hz).

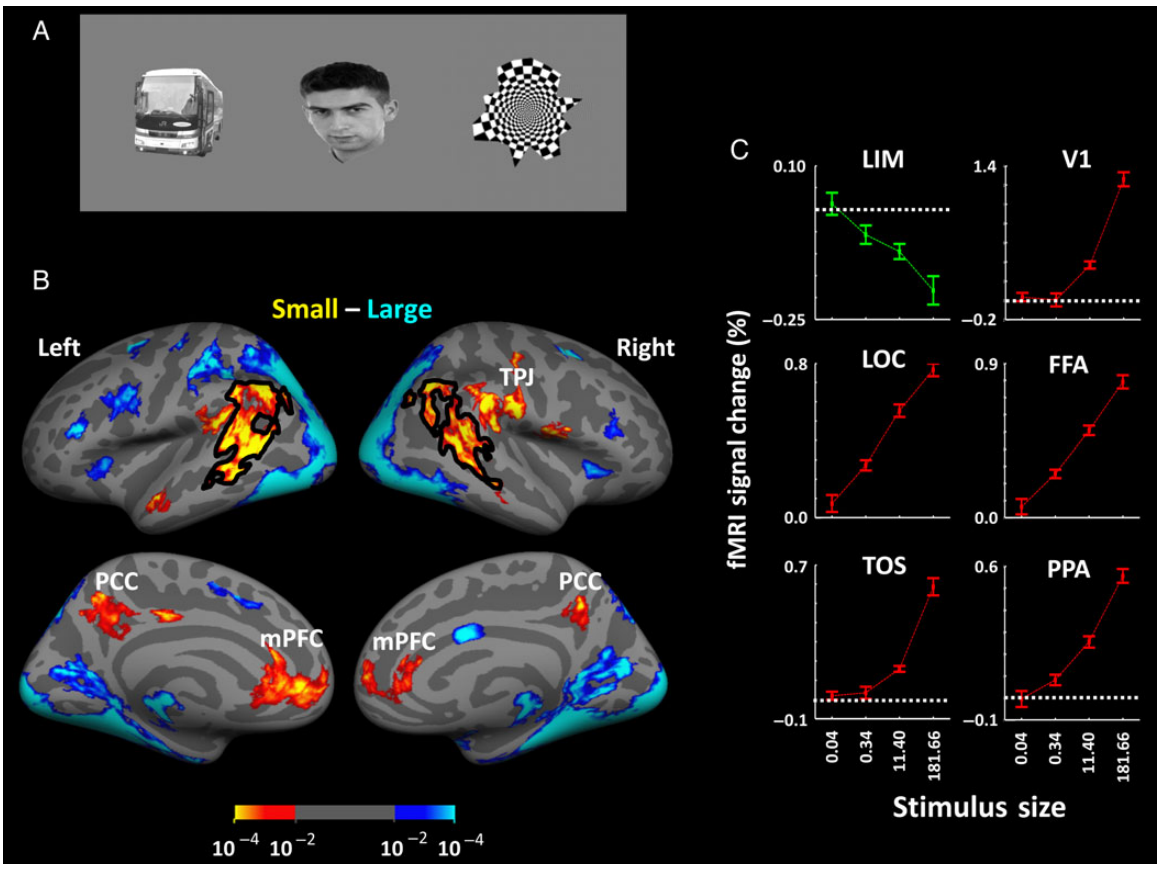

Figure 1. Stimulus examples and results in Experiments 1A and 1B. Stimuli consisted of everyday objects, faces, and geometrical shapes (*A*), presented within different blocks. (*B*) The group-averaged activity maps from lateral (top) and medial (bottom) views. Preferential responses to either large (blue to cyan) or small (red to yellow) stimuli are based on *P*-values, using random-effect analysis, corrected for multiple comparisons. (*C*) The results of ROI analysis in LIM, in comparison with the responses in well-established visual areas including V1, FFA, LOC, TOS, and PPA. Error bars indicate 1 standard error of the mean.

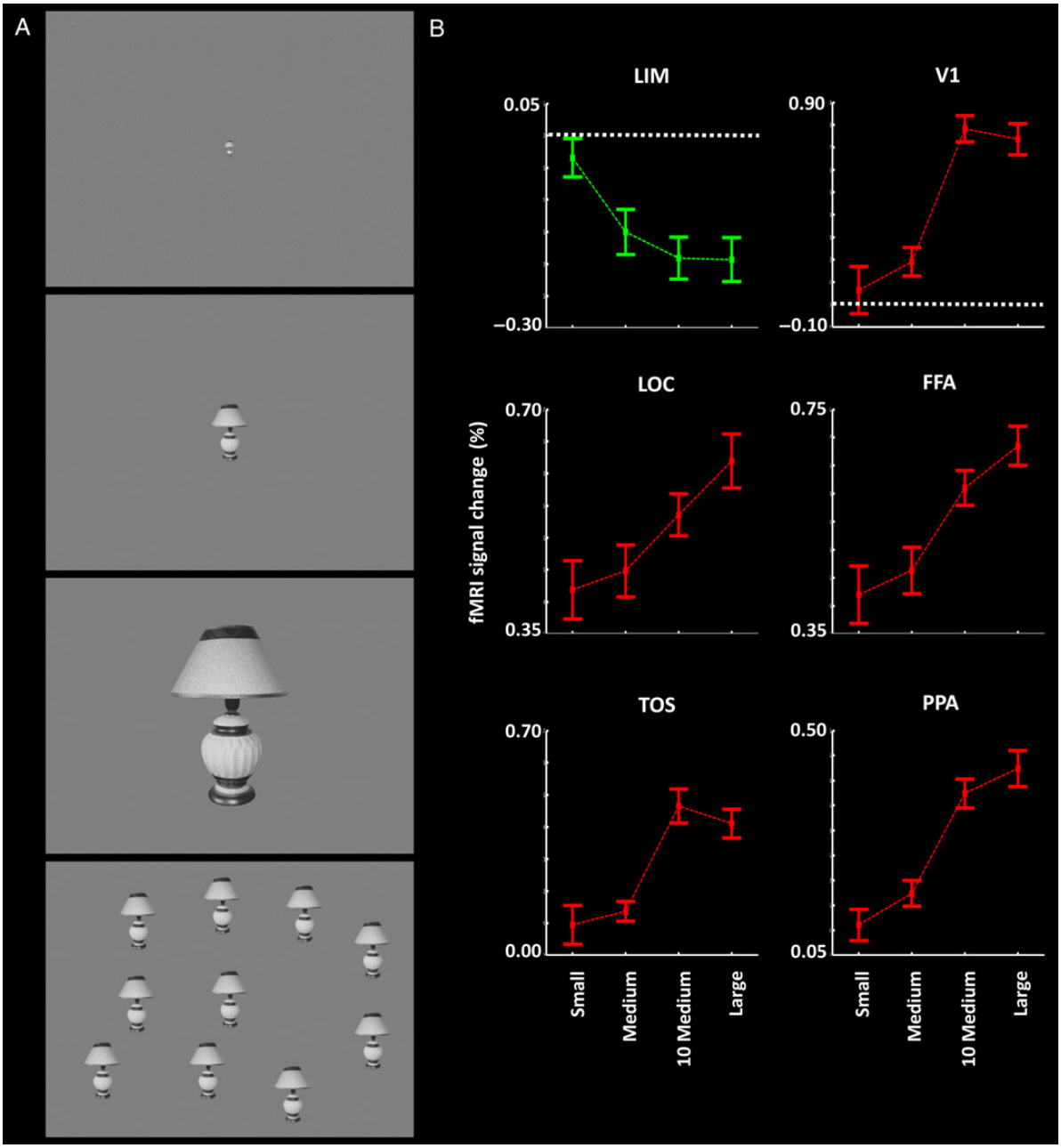

Figure 2. (A) Stimulus examples and results in Experiment 2. Stimuli were single small, medium, large, and multiple medium faces and nonface objects, independent of those used in Experiment 1 (see Methods). (*B*) The results of group-averaged activity analysis in LIM and well-established visual areas. Other details are similar to those in Figure 1.

Tasks. *Experiments* 1–3. To minimize possible variations in the level of attention across trials, subjects were instructed to detect a small translucent target dot that was presented briefly in any location on the screen, during concurrent central fixation. Target translucency (effectively, local contrast) was adjusted automatically using a staircase method converging on an accuracy of 75% correct.

Experiment 4A. In each run, subjects were instructed to either detect a change in the central fixation spot (50% of blocks) or perform a more spatially distributed dot-detection task as in Experiments 1–3. Task order was pseudo-random. For both tasks, the level of task difficulty was controlled by incrementally adjusting the color or luminance contrast of the target dot, such that response accuracy converged to 75%.

Experiment 4B. Subjects were required to detect a luminance-varying dot that was presented at a range of unpredictable locations. At the beginning of each block, subjects were cued with a message on the screen (4 s duration) indicating that the target dot appeared within ether: 1) a central disk (i.e., 0–1° radius) or 2) a mid-eccentric ring (1–10°), or 3) the sum of spatial extents 1 and 2 (0–10°). A staircase method was used to control the dot contrast so that the subject's detection accuracy converged to 75% correct across all conditions. Subjects had adequate time to practice

prior to the scans, and the experiment started when subjects felt confident about task performance.

Imaging Procedure

All human subjects were scanned in a horizontal 3T scanner (Siemens Tim Trio). Gradient echo EPI sequences were used to acquire functional images (TR 2000 ms, TE 30 ms, flip angle 90°, 3.0 mm isotropic voxels, and 33 axial slices). In the fMRI scans, the field of view included the whole brain, for all subjects. In all experiments, each subject participated in 12 runs and each run included 12 blocks. The same parameters were used for the resting state scans (6 min duration) during which subjects were required to close their eyes and lie still (i.e., in a resting state). A 3D MP-RAGE sequence (1.0 mm isotropic) was also used to acquire high-resolution anatomical images from the same subjects, for use in surface reconstruction.

Experiments with Nonhuman Primates

Subjects

Three adult macaque monkeys (*Macaca mulatta*; 4–7 kg; 1 female [M3]) were used. Animal care and experimental procedures conformed to the European and NIH guidelines and were approved by the local ethical committee. The animals were pretrained on a continuous fixation task and prepared for awake, contrast-agent enhanced fMRI experiments, as described previously (Vanduffel et al. 2001). Two monkeys were also trained on a second task, based on dot detection (Experiment 7B).

Stimuli. Images included faces (20 images), nonface everyday objects (40 images) and irregular shapes (20 images), identical to those used in Experiment 1A. In each scan session, trials were blocked according to stimulus category (i.e., faces vs. nonface objects vs. irregular shapes) and size (i.e., small vs. large; 0.34 vs. 67.33 degrees^2, respectively). Twenty-eight images were presented during each block, and each image was presented for 1 s.

Stimuli for the independent face localizer were presented in a block design (block duration: 20 s), including 6 stimulus categories: monkey faces, monkey bodies, objects, mammals, birds, and fruits (further details in Popivanov et al. 2012). All stimuli had an averaged radius of 5° of the visual field. Each block included 20 different images from a single category, and each individual stimulus was presented 2 times per block for 500 ms, in pseudo-random order.

Tasks. During Experiment 7A and during acquisition of the independent face localizer data, monkeys were rewarded with water-diluted juice for maintaining fixation within a square-shaped central fixation window (typically, 2° × 2° in size) surrounding the fixation spot.

In Experiment 7B, the same stimuli were shown in exactly the same block design, compared with Experiment 7A. During this task, each animal was required to detect a small white square (0.7°–1°) that was presented at a range of unpredictable locations throughout the full extent of the screen (40° × 30°). Monkeys had to respond within 50 to 1000 ms following the appearance of the target square by releasing a lever. The size of the square was chosen so that the animals achieved a response accuracy of 80% during the scanning session.

Imaging Procedure. The animals were fixed in the "sphinx" position inside a plastic box using a MR-compatible physical head restraint (Vanduffel et al. 2001). Functional volumes were acquired in a 3T Siemens TIM Trio scanner. A gradient echo EPI sequence was used to acquire functional images (TR 2000 ms, TE 17 ms, flip angle 75°, 1.25 mm isotropic voxels, and 40 axial slices). For monkey M1 and M2, we increased the scan sensitivity by using a gradient insert coil (Siemens AC88) with a gradient echo EPI sequence (TR 1400 ms, TE 10 ms, 1.25 mm isotropic voxels, and 40 slices). Functional data were collected with a coil (8-channel, receive only, phased-array coil with a local radial transmit coil). Immediately prior to each scanning session, an iron oxide contrast agent (SInerem, Guerbet) was injected into the femoral/saphenous vein (8–11 mg/kg). Each monkey scan session included 7–16 functional runs, and each run included 36 blocks (block duration 28 s.). For monkey M3, only small and large stimuli were presented, and each functional run consisted of 18 blocks. Each monkey was scanned for 3–8 sessions in Experiment 7A. Monkeys M1 and M2 were scanned for 2–3 sessions in Experiment 7B, and data for each experiment were averaged together. As in the human task, all monkey subjects were required to fixate a small (0.1° diameter) spot at the center of the display screen, near-continuously. Eye position was monitored using an infrared pupil tracking system (ISCAN, Inc.).

Data Analysis

Functional and anatomical data from both human and monkey subjects were preprocessed and analyzed using FreeSurfer and FS-FAST (version 5.3; http://surfer.nmr.mgh.harvard.edu/ (Fischl 2012). For each human and monkey subject, we reconstructed the cortical surface based on the high-resolution anatomical data (Fischl et al. 1999). All functional images were corrected for motion artifact and then spatially smoothed using a 3D Gaussian kernel (2.5-mm HWHM in humans and 1-mm HWHM in monkeys), and normalized across scans. To estimate the intensity of the hemodynamic response, a model based on a γ function was fit to the fMRI signal, and then, the average signal intensity maps were calculated for each condition (Friston et al. 1999). Voxel-wise statistical tests were conducted by computing contrasts based on a univariate general linear model. Finally, the significant levels were projected onto the inflated/flattened cortex after a rigid co-registration of functional and anatomical volumes.

To generate group-averaged maps for human subjects, functional maps were spatially normalized across sessions and across subjects using Freesurfer. Next, activity within each individual's brain was spatially transformed onto the averaged human brain using a spherical transformation (Fischl et al. 1999) and averaged using random-effects models (Friston et al. 1999).

For monkeys, all functional maps were spatially normalized across sessions and then spatially transformed onto the averaged monkey brain using a spherical transformation (Fischl et al. 1999). An averaged monkey brain was generated based on an independent set of animals (Nasr et al. 2011). Details of this procedure are reported elsewhere (Fischl et al. 1999). For each animal, activity maps were then averaged using fixed effects models (Friston et al. 1999) and overlaid on the average monkey brain. Details of this procedure are given elsewhere (Nasr et al. 2011).

ROI Analysis

For each human subject, we defined regions of interest (ROIs) for the scene-selective areas parahipocampal place area (PPA), transverse occipital sulcus (TOS), and RSC, and retinotopic borders, based on independent localizing stimuli (see above) at a threshold level "of" $P < 10^{-4}$. In all analyses, fMRI activity for each condition was measured relative to the activity during presentation of a uniform gray stimulus (baseline). To test the effect of independent factors, we applied a repeated-measures ANOVA, with Greenhouse–Geisser correction whenever the sphericity assumption

was violated. Subsequent comparisons between individual conditions were based on paired-sampled *t*-tests.

Group-averaged activity maps showed that all effects were generated bilaterally, without any apparent difference between left and right hemispheres. Thus, activity from both hemispheres was averaged in all ROI analyses, to strengthen the power of the statistical tests.

Functional Connectivity Analysis

Details of the functional connectivity analysis are reported elsewhere (Nasr et al. 2013). Briefly, for each subject, we removed sources of variance of noninterest including all motion parameters measured during the motion correction procedure, the mean whole-brain signal, the mean signal from the lateral ventricles, and the mean signal from a region within the deep cerebral white matter. Then, we extracted the mean BOLD signal time course for each region of interest (ROI). The correlation coefficient for each of these time courses was computed with the time course for every voxel in the brain and then converted to z-values. Whole-brain z-maps were then subjected to random-effects analyses to measure statistical significance across participants at the group level. All analyses used Freesurfer (Fischl 2012).

Results

Experiment 1: A Size-Dependent Activity Decrease in Lateral Intermediate Cortex

Experiment 1A: Small vs. Large Stimuli

To test for hypothetical cortical regions in which activity decreased in response to retinally larger (compared with smaller) visual stimuli, we measured fMRI activity in 17 human subjects during presentation of small versus large stimuli (see Methods and Fig. 1A). To maintain a consistent level and distribution of spatial attention across the experimental conditions, subjects were required to perform an unrelated ("dummy") attention-requiring task during presentation of the stimuli in all experiments mentioned below, except as noted (see Methods).

Figure 1B and Supplementary Figure 1 show the resultant group-averaged activity map in response to these large versus small stimuli, based on random-effect analysis, in both hemispheres. As expected, the larger visual stimuli evoked a correspondingly stronger response throughout well-established visual cortex. Based on additional localizing scans (see Methods), these visual areas ranged from early retinotopic areas (V1/V2/V3) through higher-level category-selective areas including the fusiform face area (FFA) (Kanwisher et al. 1997; Nasr and Tootell 2012), the (PPA) (Epstein and Kanwisher 1998; Nasr et al. 2011), the TOS (Grill-Spector 2003; Dilks et al. 2013), the lateral occipital complex (LOC; Malach et al. 1995; Grill-Spector et al. 2001), and even a small visually driven site within the anterior temporal cortex (AT; Rajimehr et al. 2009; Nasr and Tootell 2012; Avidan et al. 2014). Consistent with our hypothesis, activity in the DMN core areas (i.e., PCC and mPFC) decreased in response to retinally larger (rather than smaller) visual stimuli (Fig. 1B).

In addition to the DMN core areas, this bias for smaller stimuli was also strongly evident in the posterior portion of superior temporal cortex (STC), in the vicinity of previously described LTC, which is the DMN subarea of interest here (Andrews-Hanna et al. 2010). At a threshold of $P < 10^{-2}$, we found that the cortical region showing the size-inverted response included portions of the ANG, and the posterior portion of the STS, and the superior/medial temporal gyrus. At higher thresholds, this region had a more patchy topography, centered in the STS (Talairach coordinates left: −48, −52, 8; right: 46, −45, 11). This decrease for larger stimuli was found relatively consistently in 32 of 34 scanned hemispheres (Supplementary Fig. 2) and also across runs (Supplementary Fig. 3). To distinguish this size-defined region from other functionally or anatomically defined sites in this cortical vicinity, we refer to the region of decreased responses to larger (relative to small) stimuli as the LIM region, because it is located roughly intermediate to the occipital, parietal, and temporal cortex. As a mnemonic, "LIM" can also stand for "Less (visual stimulus) Is More (fMRI activity)" (see also Anticevic et al. 2010).

Consistent with the neuroimaging studies of visual search, we also found decreased activity in response to large (compared with small) visual objects, located within the TPJ (Corbetta et al. 2000; Shulman et al. 2007) mainly in the right hemisphere. This activity decrease was centered within the posterior portion of the lateral fissure and inferior parietal surpramarginal sulcus. This activity decrease is mainly linked to filtering of task irrelevant objects during an active search task (Shulman et al. 2007).

Previous studies have reported visual face-selective activity in the human STS (e.g., Haxby et al. 2000; Fox et al. 2009) and in the nearby lateral occipital gyrus (Nasr et al. 2011). Accordingly, here we tested for functional interactions and spatial overlap between the size-related activity variation described earlier, relative to category selectivity, in LIM and neighboring areas. As a control, we independently measured the activity contrasts evoked by small versus large everyday nonface objects, faces, and geometrical patterns. Results of this control experiment showed no significant interaction in the map contrasting category- versus size-selectivity in LIM, at a threshold of $P < 0.01$. Thus, at least in these measurements, the LIM topography produced by all 3 stimuli overlapped. As an additional validation, we found that the contrast of large faces versus large objects (Supplementary Fig. 4) confirmed the expected face-selective bias in the FFA; this ruled out the possibility that the effects reported earlier were due to ineffective stimulation by these specific face and nonface objects. Further analyses of the relationship of LIM to category selectivity are described later, in Experiment 5.

Experiment 1B: Size Response Function in LIM and Visual Cortex

To define the LIM size function in greater detail, we scanned the brain activity of 12 subjects in response to objects (including face and nonface objects, independent of those used above) in which the size (surface area) was systematically varied from 0° (i.e., a uniform gray screen, used as a baseline condition) through 0.04, 0.34, 11.40, and 181.66 degrees^2, across different blocks. For each subject, the borders of LIM (i.e., the ROI) were defined using the results of the previous small versus large stimuli (see Experiment 1A, and Methods). For comparison, we also measured the size gain function in well-documented visual cortical areas V1, LOC, FFA, TOS, and PPA. All activity was measured relative to that produced during presentation of a spatially uniform gray screen.

Figure 1C shows the results. Consistent with the results in Experiment 1A, application of a 1 factor repeated-measures ANOVA to the ROI activity showed that activity in all these well-established visual areas increased significantly and progressively with increases in stimulus size ($F_{3,33} > 8.22$, $P < 10^{-3}$). In contrast, LIM showed the opposite pattern: activity decreased systematically in response to the large visual objects, compared with the smaller ones ($F_{3,33} = 15.19$, $P < 10^{-5}$).

Experiment 2: Object Size vs. Number

In the absence of other data, it could be argued that the LIM responses depend not on object size per se (e.g., the averaged

surface area), but instead on the summed extent of the visual field encompassed by the stimulus. The latter is a more generalized sensory interpretation, which is in fact more consistent with our original hypothesis. That latter idea predicts that increases in either the number of objects, or the size of objects, should both produce decrease responses in LIM. Conversely, early retinotopic visual areas should show an opposite response; increases in either the size or number of objects (or both) should all increase the response amplitudes.

To test this idea, we measured fMRI responses in nine human subjects to presentation of face and nonface objects with the following configurations: 1) a single small object (0.51 degrees^2 visual field area), 2) a single medium object (5.59 degrees^2), 3) a single large object (55.95 degrees^2), and 4) 10 medium-sized objects presented concurrently (summed visual field area = 55.95 degrees^2) (Fig. 2A). Importantly, the total visual field area subtended by the stimuli was equivalent in the latter 2 conditions (i.e., 1 large single vs. 10 medium-sized stimuli; both totaling 55.95 degrees^2 of visual field extent). As in Experiment 1B, amplitude was calculated based on responses to the presentation of the baseline condition, a uniform gray (i.e., a stimulus of 0 degrees^2).

Consistent with the results in Experiments 1A and 1B, we found a significant decrease in LIM activity when the size of a single object was increased (Fig. 2; $F_{2,16} = 6.95$, $P < 0.01$). Importantly, this experiment also showed that the LIM response to a single large object did not differ significantly from its response to 10 medium-sized objects ($t_8 = 0.96$, $P = 0.37$), when both stimuli had equivalent summed visual field area. This result suggests that LIM activity inversely reflects the visual field extent occupied by the sum of the tested visual stimuli on the screen at a given time, rather than the size of a given object per se. This more general interpretation is consistent with our basic hypothesis that stronger visual stimulation (e.g., increases in either the size or number of visually presented objects) produces decreased activity in DMN-related areas. For clarity, we nevertheless refer to the main experimental value as "size" (rather than "visual field area") below, when the experimental manipulations were based on the size of a single object at a given time.

Consistent with the results in Experiments 1A and B, occipital and inferior temporal visual areas (including V1, FFA, LOC, TOS, and PPA) showed a significantly higher response to progressively larger objects, compared with smaller objects ($F_{2,16} > 8.31$, $P < 0.01$). Among these comparison visual areas, LOC ($t_8 = 2.39$, $P = 0.04$) and FFA ($t_8 = 2.17$, $P = 0.06$) showed a marginally higher response to a single large object, compared with 10 medium-sized objects of equal summed visual field area. However, the responses evoked by a single large object vs. 10 medium size objects were not differentiable in the other tested visual areas ($t_8 < 1.46$, $P > 0.18$). Thus, generally, responses in well-established visual cortex scaled with variations in visual field area, with a response sign opposite to that in LIM.

Experiment 3: Visual Field Position

In Experiments 1A and 1B, the stimuli were centered in the visual field; thus, the "size" effect was not accompanied by co-variations in averaged stimulus eccentricity (i.e., angular distance from the center of gaze). Nevertheless, it might be argued that 1) the decreasing or increasing object sizes recruited a narrower or broader range of eccentricities, biased toward the foveal/peripheral regions in the visual field (respectively) and that 2) somehow this retinotopic variation influenced (or even produced) the apparent size effect. To address this overall possibility, Experiment 3 tested the LIM size function in 13 human subjects across variations in averaged visual field eccentricity (see Methods and Fig. 3A,B).

Figure 3C shows the activity measured in LIM and additional control areas. Application of a three-factor repeated-measures ANOVA (size [0.35 vs. 70.50 degrees^2], eccentricity [10° vs. 15° vs. 20°], and laterality [ipsilateral vs. contralateral]) to the activity in LIM confirmed a significantly decreased response to larger (compared with smaller) stimuli ($F_{1,12} = 28.24$, $P < 10^{-3}$). We did not find a significant effect of stimulus eccentricity ($F_{2,24} = 1.11$, $P = 0.35$) or laterality ($F_{1,12} = 0.63$, $P = 0.44$) on the level of LIM activity. However, the interaction between the effects of size and laterality was significant ($F_{1,12} = 11.59$, $P < 0.01$), and the effect of size on LIM activity was stronger in the contralateral rather than the ipsilateral hemisphere. Thus, the activity decrease in LIM in response to larger stimuli was largely independent of stimulus eccentricity, within the range tested here (5.25°–24.75° [i.e., minimum–maximum eccentricities]).

As expected, activity in established visual areas increased significantly when stimuli were presented either at larger size ($F_{1,12} > 11.03$, $P < 0.01$) or nearer to the fovea ($F_{2,24} > 13.97$, $P < 10^{-3}$) (Fig. 3C). Moreover, unlike the size effect in LIM, the effect of size in V1 ($F_{2,24} = 14.07$, $P < 10^{-4}$), LOC ($F_{2,24} = 5.23$, $P = 0.01$, FFA ($F_{2,24} = 3.97$, $P = 0.03$), and TOS ($F_{2,24} = 4.04$, $P = 0.03$) but not in PPA ($F_{2,24} = 1.18$, $P = 0.32$) was larger when stimuli were located nearer rather than farther from the foveal representation. Also, consistent with known functional properties, all tested visual cortical areas showed a stronger response in the contralateral hemisphere, compared with the ipsilateral hemisphere ($F_{1,12} > 8.46$, $P < 0.01$).

Experiment 4: Central vs. Spatially Distributed Attention

Experiment 4A: Comparison Across Tasks

Experiments 1–3 showed a systematic and inverse influence of visual stimulation on LIM responses, using an independent task to stabilize possible co-variations in attention. To complement these tests of sensory-driven activity, we next tested whether experimental manipulations in spatial attention would influence LIM activity.

Eleven human subjects were scanned during presentation of large versus small visual objects. Across different scan blocks, subjects were cued to detect changes in contrast (color or luminance; see Methods) in a target dot, which was located either 1) at the center of the screen, or 2) distributed unpredictably and randomly across the display screen (i.e., similar to the dummy dot-detection task used in Experiments 1–3). Thus, in these 2 tasks, spatial attention was either distributed across the screen, or focused centrally. The level of difficulty for both tasks converged to 75% using a staircase method (see Methods).

Figure 4 shows the resultant group-averaged brain activity in response to large versus small stimuli during spatially distributed (Fig. 4A) versus foveally centered (Fig. 4B) attention. We found that the expected size-dependent decrease was greatly reduced during central attention, compared with spatially distributed attention. Application of a two-factor repeated-measures ANOVA to the activity measured within LIM (Fig. 4C) showed a significant effect of task ($F_{1,10} = 32.28$, $P < 10^{-3}$), stimulus size ($F_{1,10} = 22.02$, $P < 10^{-3}$), and a significant interaction between the effects of stimulus size and task ($F_{1,10} = 32.30$, $P < 10^{-3}$). Although additional factors may contribute (see below), these results suggest that spatially distributed attention enhances the size-dependent response in LIM.

Again, the pattern of activity in well-established visual areas was quite different than the pattern of activity in LIM. In visual

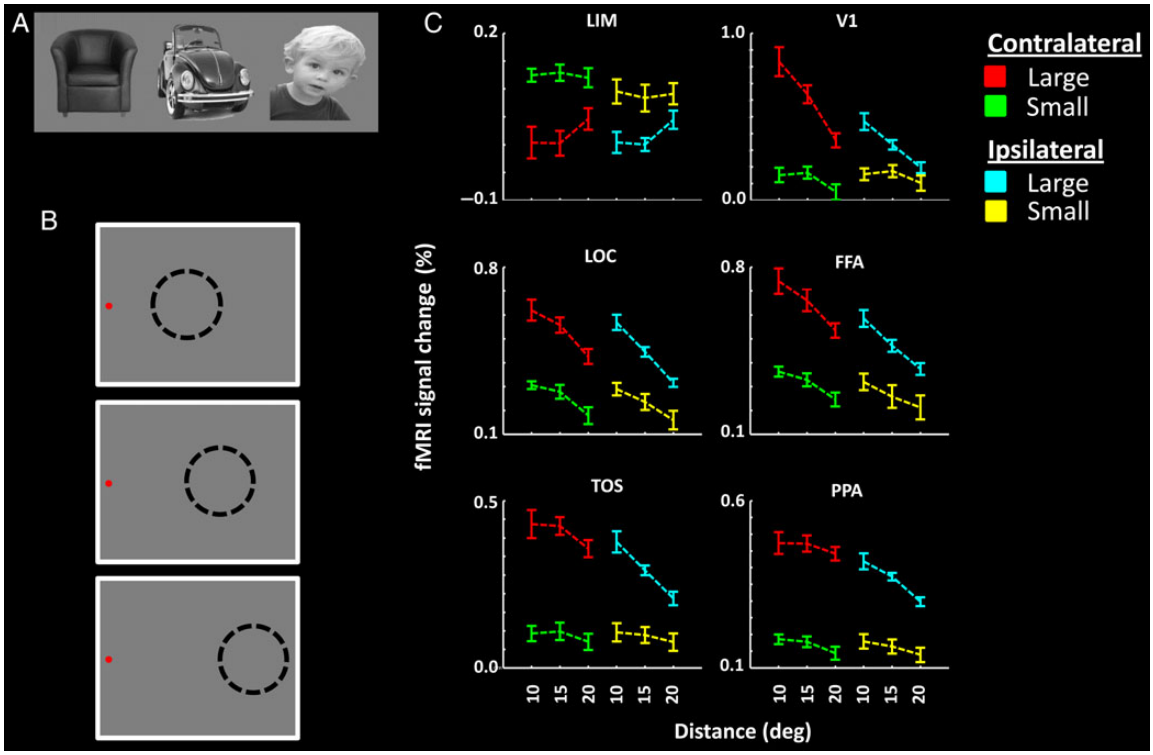

Figure 3. Stimuli and results in Experiment 3. Stimuli were everyday objects and faces, independent of those used in Experiments 1 and 2 (*A*). Stimuli were presented in the periphery of the visual field, and subjects were instructed to maintain fixation on a target presented either on the left (*B*) or the right side of the screen. The distance between the stimulus (presented by dashed circles) and the fixation spot was systematically varied across blocks. (*C*) The results of ROI analysis. The eccentricity of the stimulus center is indicated on the *x*-axis. Other details are as in Figure 1.

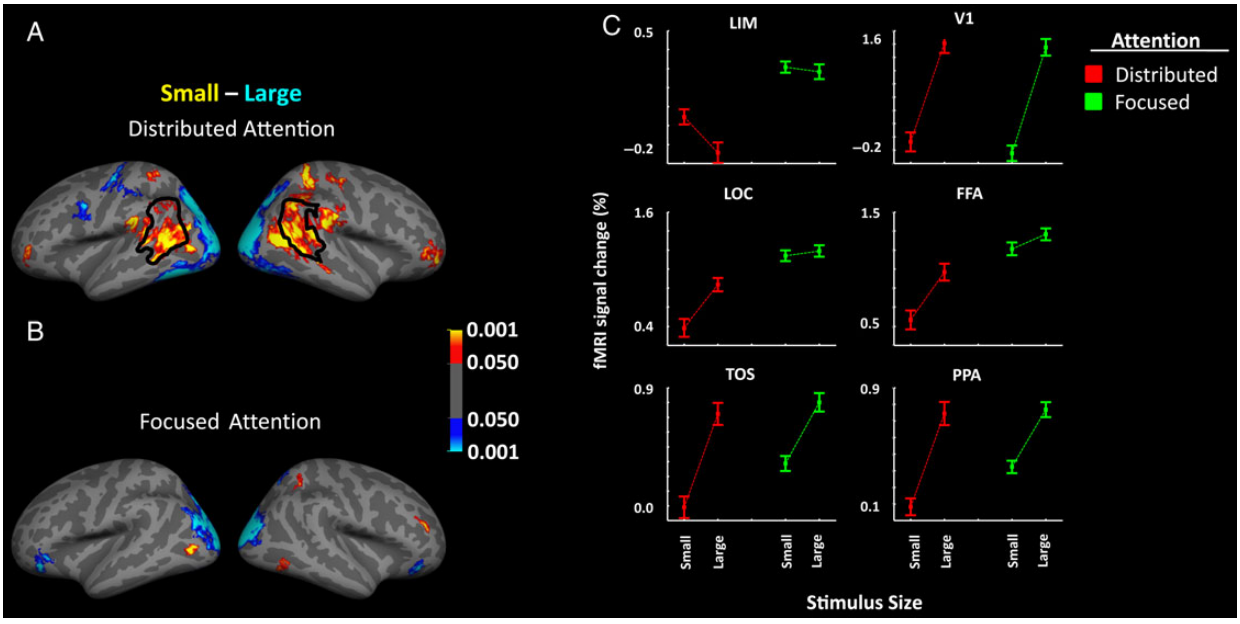

Figure 4. Group-averaged activity maps showing areas that responded preferentially to small (red-yellow) or large (blue-cyan) stimuli, during spatially distributed (*A*) or centrally focused (*B*) attention. The border of LIM is defined based on independent scans (Experiment 1) in the same pool of subjects. (*C*) The results of the ROI analysis in LIM and in well-established visual areas. Other details are similar to those in Figure 1.

cortex, we found significantly stronger activity in response to larger compared with smaller stimuli ($F_{1,10} > 18.17$, $P < 0.01$). All tested visual areas except for V1 ($F_{1,10} > 0.49$, $P = 0.51$) showed a significant interaction between the effect of stimulus size and task ($F_{1,10} > 21.77$, $P < 10^{-3}$). However, in contrast to LIM, this interaction arose mainly from an increased response to the smaller stimuli during central rather than distributed attention. Areas FFA ($F_{1,10} > 11.05$, $P < 0.01$) and LOC ($F_{1,10} > 17.70$, $P < 0.01$) showed

a significant effect of task, but we found no significant difference between the 2 tasks in the level of activity within V1 ($F_{1,10} > 2.90$, $P = 0.12$), PPA ($F_{1,10} > 2.66$, $P = 0.13$) or TOS ($F_{1,10} = 2.37$, $P = 0.16$).

Experiment 4B: Common Task

In the above experiment, it could be argued that residual differences in the nature of the 2 tasks could have influenced the results. Therefore, we scanned 13 subjects in a control experiment during which subjects were required to detect a luminance-varying dot that was presented at a range of unpredictable locations. Those locations were confined within either: 1) a central disk (i.e., 0–1° radius) or 2) a mid-eccentric ring (1–10°) or 3) the sum of spatial extents 1 plus 2 (0–10°). Thus, spatial attention was most centered in Condition 1. In all 3 conditions, the target dot was presented on a large radial checkerboard (Supplementary Fig. 5), reversing in contrast at 1 Hz. Subjects were cued to the eccentricity range of the target dot at the beginning of each block (see Methods). Using a staircase method similar to the one in Experiments 1–3 and 4A, task performance converged to 75% correct across all conditions. LIM activity was measured relative to a baseline condition of uniform gray background (i.e., no checkerboard), during which the subjects were required to fixate the fixation spot without an explicit task (i.e., passive fixation).

Consistent with the results of Experiment 4A, we found a significant effect of the distribution of spatial attention on the LIM response level ($F_{2,24} = 3.49$, $P = 0.04$). The LIM response to the large checkerboard was reduced during the 2 conditions involving wider spatial attention (i.e., Conditions 2 and 3), compared with the more centered condition (i.e., Condition 1). Thus, despite the experimental differences between Experiments 4A and 4B, both sets of results indicate that spatially distributed attention enhances the distinctive response decrease to larger stimuli in LIM.

Experiment 5: Meta-Analysis

Numerous studies have reported category-selective activity in the vicinity of LIM, including visually driven selectivity for faces or biological motion in STS, and/or a cognitively driven site selective for ToM (for review, see Allison et al. 2000; Spreng et al. 2009; Kanwisher 2010). To relate our findings more directly to those in the literature, we co-localized the group-averaged size-selective localizer for LIM (Experiment 1) to a meta-analysis of data from the above reports, and to additional data from our laboratory.

Experiment 5A: Selectivity for Faces

Figure 5A shows the location of face- (or gaze-) selective sites reported in the literature (small solid squares; Table 1). In addition, we plotted the center of higher face selectivity in the STS, based on our data in Experiment 1A (white circle in Fig. 5A) (see also Supplementary Fig. 4). Such face-related sites were clustered in the anterior/ventral portion of LIM, within the STS. Moreover, the face-selective site in our data was located in the middle of that cluster. Thus, locations in our data were consistent with those in the literature.

Experiment 5B: Selectivity for Biological Motion

Figure 5B shows the analogous comparison of LIM to the peaks of activity that have been reported to represent biological motion (see also Table 2). In addition, we plotted the data from an additional experiment conducted in our laboratory, in which responses to point-light displays of biological motion (Johansson 1973) were contrasted with translational ("planar," a form of non-biological) motion (see Methods), using stimuli identical to those used in a previous study of biological motion (Jastorff and Orban 2009). The cluster of peaks in this biological motion meta-analysis and the peak activity in our biological motion experiment were mainly located in the STS, within the borders of LIM as defined here. However, the meta-analysis clustering for biological motion (Fig. 5B) was distributed more variably, compared with that for faces (Fig. 5A).

Experiment 5C: Selectivity for ToM

Figure 5C shows the analogous meta-analysis of published sites involved in the processing of ToM on the superior temporal gyrus. The reported ToM sites (Table 3) were located more dorsally in the superior temporal gyrus (rather than in the sulcus), but still within the borders of LIM.

Overall, the results of this meta-analysis show complementary features. On one hand, all 3 of these category-selective tests (face, biological motion, and ToM selectivity) activated sites within LIM, when LIM was defined in our experiments at a relatively low threshold (e.g., Fig. 1 [$P < 10^{-2}$]). On the other hand, the 3 different functionally defined sites appeared to be in different locations within LIM, within the limits of this meta-analysis. Thus, these results suggest that size-defined LIM may well include functionally distinct subdivisions. Previous meta-analyses also reported functional subdivisions in this general region, although they did not define LIM (e.g., Allison et al. 2000; Spreng et al. 2009; Kanwisher 2010; Denny et al. 2012).

Experiment 6: Functional Connectivity

To clarify the circuitry of LIM, Experiment 6 mapped the functional connectivity of LIM relative to that in well-established visual and DMN areas, by measuring resting-state BOLD signal fluctuations in 24 human subjects (see Methods). The seed regions for LIM and PCC were defined based on the results of Experiment 1. The seed regions for visual areas were defined based on an independent set of localizer stimuli in independent scan sessions (see Methods). To avoid uncontrolled variation between areas due to a common sensory input, subjects were instructed to keep their eyes closed throughout the functional connectivity scans.

Figure 6 and Supplementary Figure 6 show the resultant maps. Consistent with the previous reports of human STS connectivity (Yeo et al. 2011), LIM showed a strong (positive) functional connection with anterior STS. Also, as one would expect in a DMN subarea (Andrews-Hanna et al. 2010), LIM showed a strong functional connection with DMN core areas (i.e., PCC and mPFC) plus lateral frontal areas. LIM also showed a negative functional connection with parietal/insular cortex and early visual cortical areas. Consistent with the other evidence for a link between LIM and DMN-related regions, seeding of PCC revealed a strong functional connection between PCC and the dorsal posterior portion of LIM. The restriction of the connections to the dorsal posterior region of LIM is further evidence (see Experiments 5A-C) for functional subdivisions within size-defined LIM.

In contrast, the functional connections of the classic visual areas differed strikingly from those in LIM. At a threshold of $P = 10^{-2.5}$, the positive functional connections from seeds in each visual cortical area were largely limited to other areas within visual cortex. In contrast to LIM, all tested visual areas except FFA showed "negative" functional connection with DMN areas, and with the lateral frontal cortex (see also Chadick and Gazzaley 2011). However, at a lower threshold of $P < 10^{-2.5}$, many mid-level visual areas (especially MT) showed a significant positive

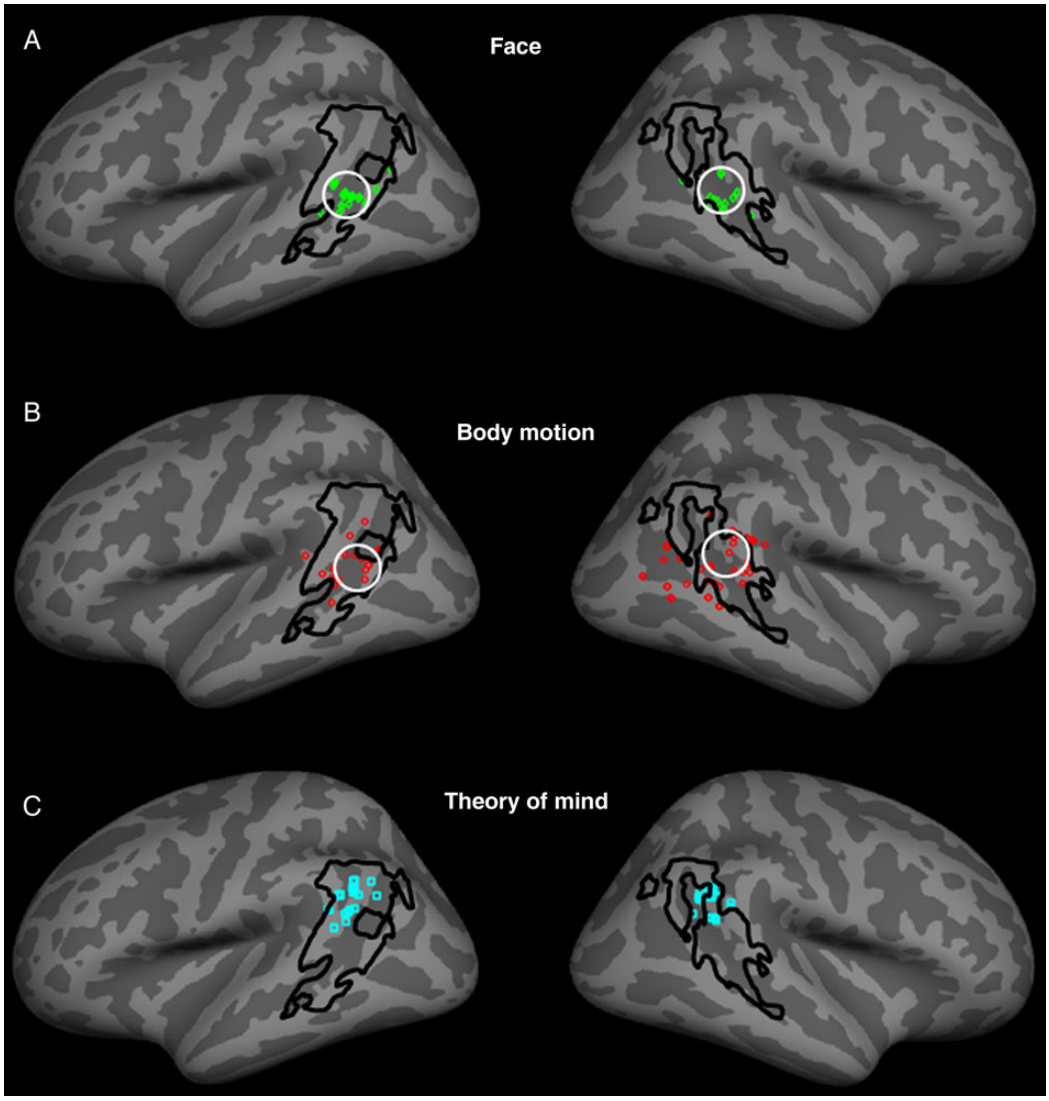

Figure 5. Co-localization of LIM relative to the reported peaks of activity in previous studies describing selectivity for faces (*A*) and biological motion (*B*) in STS (see Tables 1 and 2). The location of LIM was based on the results of Experiment 1. The peaks of activity to face- and biological motion-selective localizers in our subjects are indicated by white circles, in *A* and *B*, respectively. (*C*) The reported peaks of activity during ToM tasks, relative to the borders of LIM (see Table 3).

Table 1 Location of peaks of face-selective response within the posterior STS reported in previous studies

−53	−34	5	49	−39	9	Pinsk et al. 2009
−39	−65	17	47	−63	13	
−47	−48	8				
−50	−55	8	53	−44	4	Fox et al. 2009
−51	−52	6	51	−41	4	
−49	−61	16	50	−45	16	Hooker et al. 2003
−55	−60	10	52	−48	8	Engell and Haxby 2007
−54	−48	4	53	−45	7	Ishai et al. 2005
−56	−46	12	54	−42	8	Furl et al. 2011
−51	−49	6	46	−44	6	Avidan et al. 2014
−54	−38	6	48	−38	4	Julian et al. 2012
−57	−45	6	54	−33	3	Schultz et al. 2013
			60	−51	9	Liu et al. 2010
			48	−34	2	Thompson et al. 2007

functional connection to a small common anterior/ventral portion of LIM. This functional connection data further supported the above evidence that LIM is a heterogeneous area.

To further test this possibility, we divided LIM arbitrarily into 3 areas of roughly equal size along the anterior–posterior axis and measured the functional connection of each subdivision relative to the rest of the brain (Supplementary Fig. 7). The results showed clear differences in functional connections between these 3 subdivisions of LIM (Fig. 7).

Specifically, the posterior third of LIM showed the highest level of positive functional connection with the DMN main hubs (i.e., PCC and mPFC). It also showed a strong "negative" functional connection with the mid-level occipital temporal visual areas, plus dorsal anterior cingulate cortex (dACC), and central and insular cortex. Despite the low threshold used in this analysis ($P < 0.05$), the negative functional connection between the posterior LIM and area V1 was limited to the peripheral (not including the foveal) representation in V1.

The functional connections of middle/anterior portions of LIM showed 4 major differences relative to those of posterior LIM. First, middle, and anterior LIM showed weak (or no) functional connection to dACC, or central or insular cortex. Second, middle, and anterior LIM showed weaker functional connections

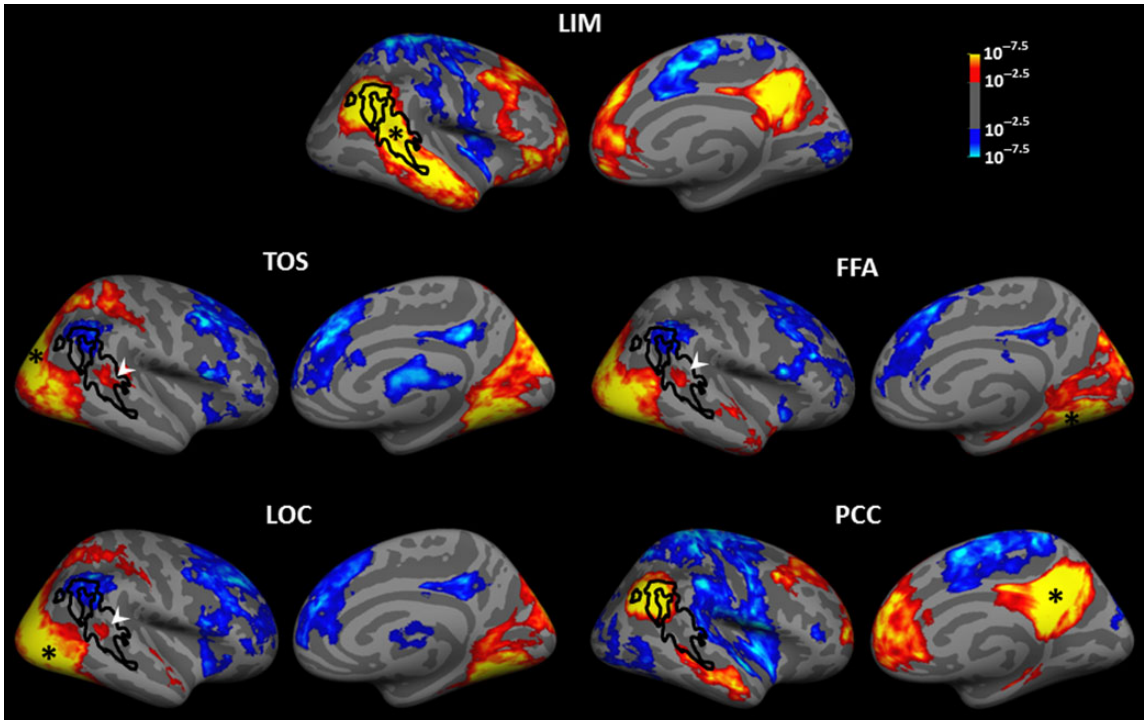

Figure 6. Functional connectivity of LIM and adjacent visual areas, including TOS, LOC, and FFA, illustrated in the right hemisphere. The bottom panel shows the functional connectivity of PCC. Black lines show the borders of LIM. The white arrowhead indicates the anterior/ventral part of LIM, which shows a positive functional connection with the FFA, TOS, and LOC. In each panel, black asterisks indicate the center of the seeded area.

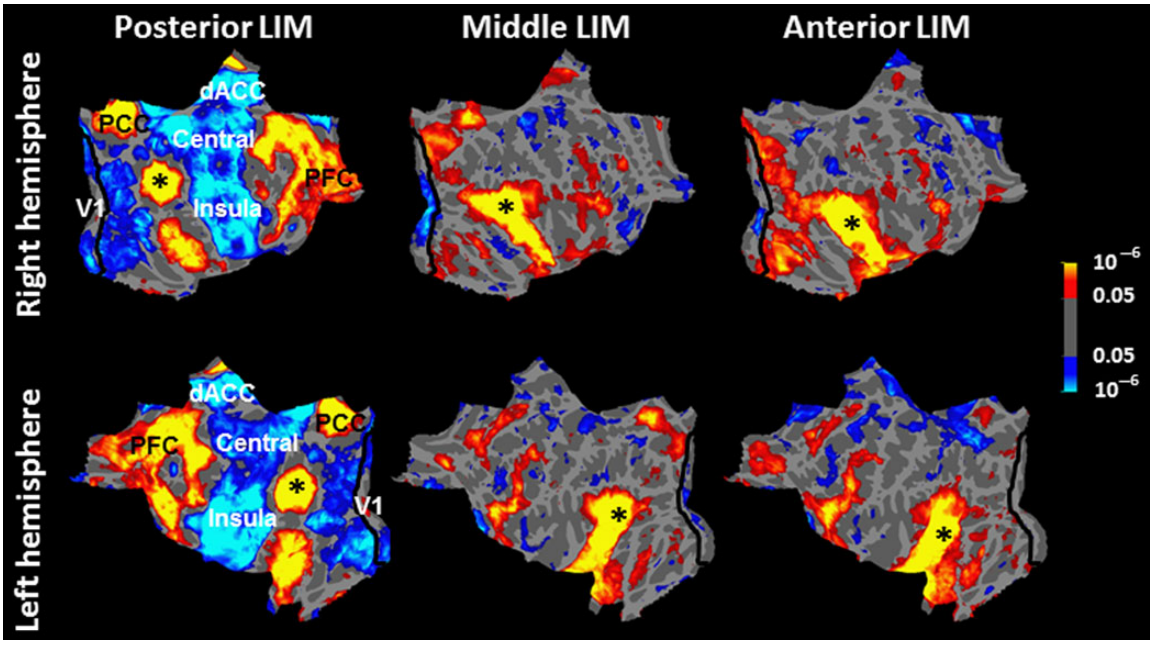

Figure 7. Functional connectivity map of posterior (left); middle (center) and anterior (right) LIM, overlaid on flattened right (top) and left (bottom) hemispheres. Asterisks mark the center of the seeded area in each map. Probabilistic borders of area V1 (Hinds et al. 2008) are also indicated with a black line.

with DMN main hubs (i.e., PCC and mPFC) compared with the posterior LIM. Third, anterior/middle portions of LIM showed a "positive" (rather than "negative") functional connection with mid-level visual areas. Fourth, anterior, and middle portions of LIM showed "negative" functional connection to area V1. However, in contrast to the posterior LIM, the latter functional connection was mainly with the foveal rather than the peripheral portion of this retinotopic area. The latter 2 differences were more prominent in the right hemisphere. Notably, this negative functional connection with area V1 was found only in LIM, and none of the tested visual areas showed such a negative functional connection with area V1.

Table 2 Location of peak of biomotion-selective response within the posterior STS reported in previous studies

−39	−59	15	47	−56	15	Beauchamp et al. 2003
−41	−52	11	46	−49	12	Grossman and Blake 2002
−45	−56	14	59	−42	19	Carter and Pelphrey 2006
−45	−58	8				Schnell et al. 2007
−46	−54	14				Saygin et al. 2004
−47	−61	23	42	−58	20	Schubotz and von Cramon 2004
−48	−46	4	54	−50	4	Calvert and Campbell 2003
−48	−46	6	51	−54	10	Grosbras and Paus 2006
−51	−44	10	63	−36	13	Grèzes et al. 2003
−52	−50	14	58	−42	6	Dubeau et al. 2001
−52	−59	9	59	−37	20	Gobbini et al. 2007
−53	−42	13				Pierno et al. 2006
−54	−44	12				Villarreal et al. 2008
−55	−47	2	55	−54	6	Costantini et al. 2005
−59	−42	9	52	−36	5	Pelphrey et al. 2005
			38	−58	14	Hamilton and Grafton 2006
			44	−68	10	Vaina et al. 2001
			46	−46	11	David et al. 2008
			50	−43	4	Wheaton et al. 2004
			50	−48	2	Gazzola et al. 2006
			50	−40	20	Gazzola et al. 2007
			52	−37	6	Sakreida et al. 2005
			52	−61	8	Morris et al. 2005
			55	−51	27	Ramnani and Miall 2004
			56	−46	13	Peuskens et al. 2005
			57	−41	21	Peelen et al. 2006
			57	−45	16	Bidet-Caulet et al. 2005
			62	−37	21	Leslie et al. 2004
			63	−44	2	Santi et al. 2003
			63	−39	6	Makuunchi 2005
			64	−52	5	Johnson-Frey et al. 2005
			64	−40	9	Ohnishi et al. 2004

Table 3 Location of peak of ToM-related response within the posterior STS reported in previous studies

−42	−61	27	55	−49	30	Young et al. 2007
−48	−54	30	53	−54	28	Perner et al. 2006
−53	−57	22	53	−49	19	
−49	−59	21				Heekeren et al. 2003
−55	−59	20				Heekeren et al. 2005
−63	−47	23	64	−49	26	Kobayashi et al. 2007
−59	−50	14				Robertson et al. 2007
−50	−58	20	58	−52	22	Dodell-Feder et al. 2011
−54	−50	18	52	−48	20	Sebastian et al. 2011
−53	−59	24	57	−56	26	Gobbini et al. 2007
−50	−64	35				Prehn et al. 2008
−51	−55	27	55	−51	28	Young and Saxe 2008
−50	−54	28				Saxe and Powell 2006
−56	−52	26	58	−52	28	Young et al. 2010
−54	−60	21	51	−54	27	Saxe and Kanwisher 2003
			34	−51	25	Sommer et al. 2007
			41	−47	22	Moll et al. 2002
			46	−49	19	Greene et al. 2004
			60	−46	22	Gallagher et al. 2000
			53	−51	19	Hynes et al. 2006
			53	−48	27	Mitchell 2008

Experiment 7: LIM in Macaque Monkeys

To test for evidence of an LIM homolog in macaques, we first predicted the location of LIM in the macaque cortical map, based on the topographic projection of corresponding visual cortical areas in human cortex using Caret (Van Essen et al. 2001). This projection was accomplished using a landmark-based deformation. Tethering points included both functionally mapped areas (V1, V2, and MT) plus anatomical landmarks (the central sulcus, rhinal sulcus, and sylvian fissures). First, human and monkey brain landmarks were registered precisely to each other. Then, the remaining cortical areas were mapped from the human map to the macaque, as constrained by the tethering areas and the cortical surface limits (for further details, see Van Essen et al. (2001)). This approach has been used previously to predict the location of presumptively common visual cortical areas including lateral occipital complex and anterior face areas, by translating map information from humans to macaques, and vice versa (e.g., Tsao et al. 2003; Van Essen 2005; Rajimehr et al. 2009). That projection is shown in Figure 8. Based on this mapping approach, a hypothetical macaque homolog of LIM should be located immediately anterior to macaque MT+ (i.e., anterior to MSTd; e.g., Nelissen et al. 2006).

Experiment 7A: Fixation Only

In our first test, we scanned 3 macaque monkeys whereas they fixated a small target spot, during presentation of a diagnostic subset of the stimuli used in Experiment 1A (see Methods). Stimuli were blocked according to size (large vs. small) and image category (faces vs. nonface objects), in a 2 × 2 design.

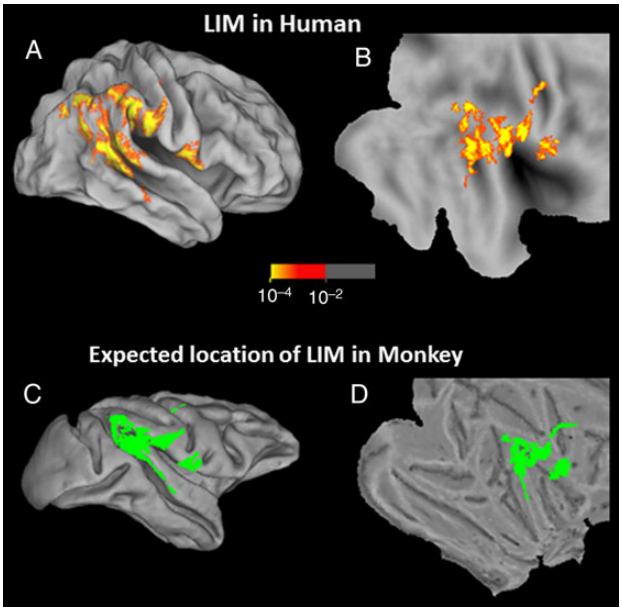

Figure 8. Topographic projection of the human data to predict the location of putative LIM in macaque monkey, based on warping of the cortical surfaces. The top 2 panels show the group-averaged activity map showing the inverted size bias (red-through-yellow) based on the results from Experiment 1, in inflated (*A*) and flattened (*B*) views of the human brain. The bottom 2 panels show the predicted location of LIM in the macaque, in corresponding inflated (*C*) and flattened (*D*) views of the macaque brain, shown in solid green.

Results of this experiment are shown in Figure 9. Unlike the results in human subjects, we did not find a sizable cortical region showing decreased fMRI response to retinally large (compared with small) stimuli, in the cortical location predicted by the cortical projection of human LIM onto macaque cortex. That is, this experiment did not reveal any obvious homolog of human LIM, in any of the 6 hemispheres tested.

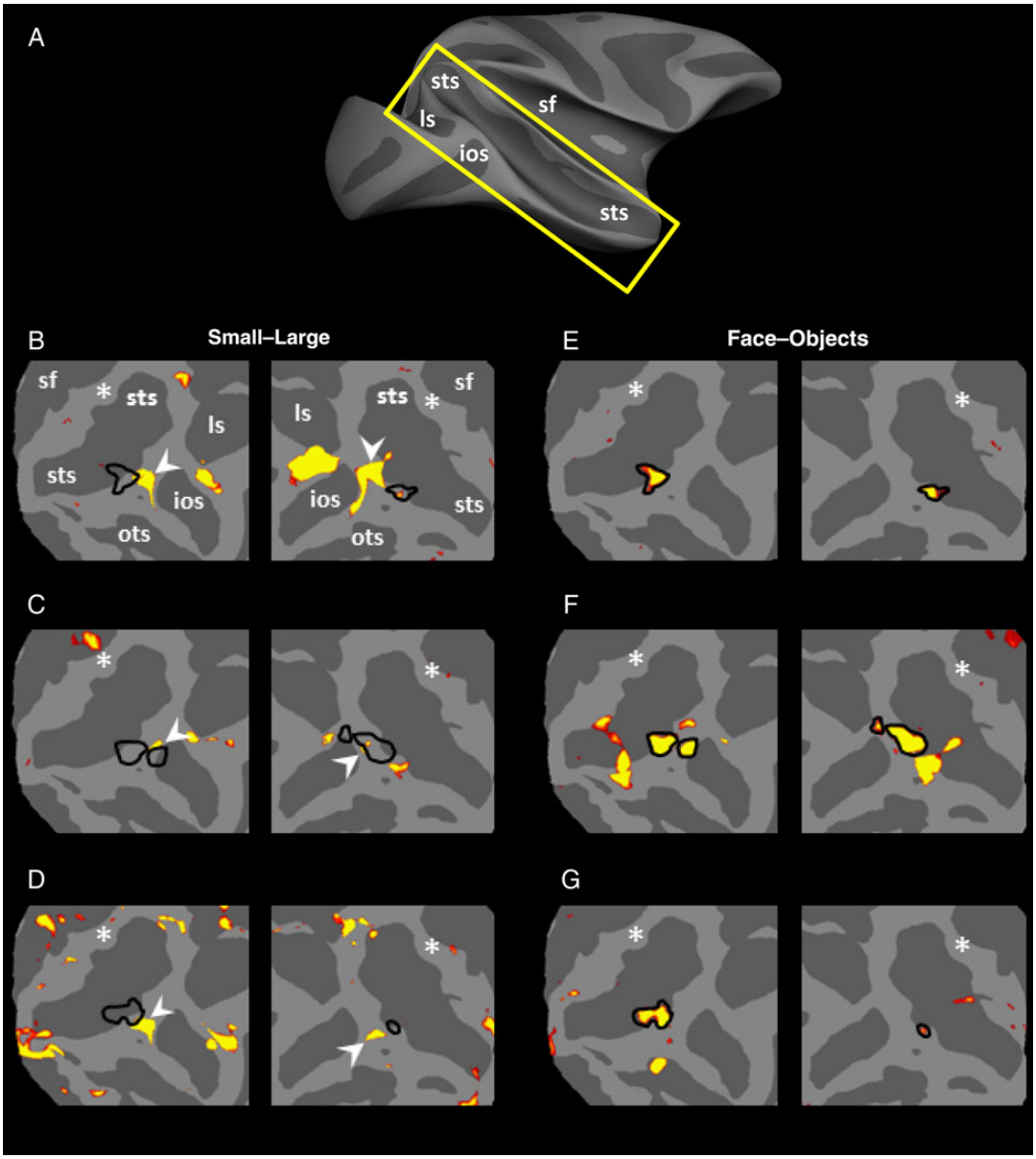

Figure 9. Results of Experiment 7A in 3 monkeys. (*A*) The approximate location of insets on a monkey brain with anatomical landmarks highlighted on the map. (*B–D*) Regions that responded preferentially to small (rather than large) stimuli during passive fixation (red-through-yellow). Stimuli were a subset of stimuli used in Experiment 1, which included faces and nonface everyday objects. The locations of small functional patches that are functionally similar to human LIM are indicated by white arrows. Based on the cortical projection, the predicted activity peak of LIM is indicated with a white asterisk. Black lines (*E–G*) show the borders of the posterior face-selective patches located in the same hemispheres. STS, superior temporal sulcus; LS, lunate sulcus; IOS, inferior occipital sulcus; OTS, occipital temporal sulcus; SF, sylvian fissure.

However, we did observe small regions located outside the projected region of LIM, which showed "functional" similarities to human LIM. It could be argued that such small patches represent "proto-homologues" of LIM, except for their anomalous location outside the LIM projection region (Fig. 8). These potential proto-LIM patches were found in all 6 hemispheres (Fig. 9), based on the large versus small localizer.

In the same 3 animals, the main ("middle" or "posterior") face patch (Pinsk et al. 2009; Rajimehr et al. 2009; Bell et al. 2011; Nasr et al. 2011) was also localized based either on the same stimuli used in this test (in all hemispheres) or based on a different set of stimuli (in 2 hemispheres; Supplementary Fig. 8). In each of these 6 hemispheres, 1 of these proto-LIM patches was located adjacent to the monkeys' posterior face-selective patch (Pinsk et al. 2009; Rajimehr et al. 2009; Bell et al. 2011; Nasr et al. 2011).

In addition, we found a patch that was located in the confluent foveal representation of V1/V2, in 5 of the 6 hemispheres in which neural response levels decreased in response to the large compared with the small stimuli. In a retrospective analysis, we noted that some of our human subjects (12 of 34 tested hemispheres) showed an analogous patch of activity in the foveal representation of V1/V2, at low thresholds. Based on this and previous fMRI studies (e.g., Tootell et al. 1998), such foveal V1/V2 patches likely reflect a minor variability in fixation stability across conditions.

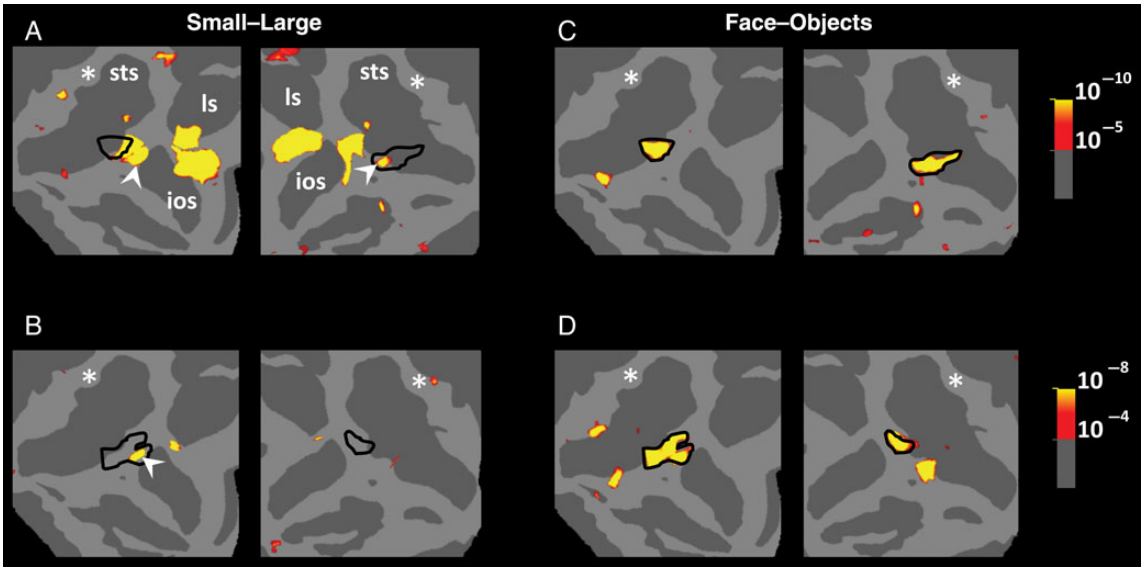

Figure 10. Results of Experiment 7B in 2 monkeys. *A* and *B* show activity patches that responded preferentially to small rather than larger stimuli during an active task comparable with the dot-detection task used in humans. The location of the posterior face-selective patches in the same hemispheres is shown in *C* and *D*. Other details are similar to those in Figure 8.

Experiment 7B: Fixation with Spatially Distributed Attention

Human experiments 4A and 4B suggested that the response difference to small versus large objects (i.e., the LIM localizer) is stronger during distributed (compared with more centralized) attention. Thus, if an LIM homolog exists in macaques, its' activity might be enhanced by constraining the monkey's task to distribute attention more uniformly across the stimulus display.

To test this idea, we conducted further scans in 2 of the monkeys using the same stimuli used in Experiment 7A, plus an additional task constraint. The monkeys were trained to perform an additional task (similar to the task performed by humans in Experiments 1–3) that required monkeys to distribute their attention across the screen, while concurrently maintaining their fixation at the central fixation spot (see Methods).

Figure 10*A* shows the resultant activity maps. Consistent with the results of Experiment 7A, we did not find any obvious homolog of LIM in the predicted cortical region. However, again, these experiments revealed a preference for small rather than large objects in the same small patches localized in Experiment 7A, in 3 of 4 hemispheres. Figure 10*B* also confirms that these patches were located immediately posterior to the monkey face patches, as one would expect from transitivity.

Discussion

Our results demonstrate that a specific cortical region ("LIM," located just anterior to classic dorsal visual cortex) is progressively and consistently de-activated by corresponding increases in stimulated visual field extent. Additional evidence suggests that LIM is linked to visual cortex mainly through indirect and higher order circuits, including the DMN core areas.

To What Extent is LIM Involved in Visual Processing?

Perceptually, larger objects are more easily detectable and recognizable compared with smaller ones (Jolicoeur 1987). Consistent with this perceptual effect, we found that larger (i.e., more salient) stimuli evoked stronger activity relative to smaller stimuli (Figs 1–3), throughout well-established visual cortex, including early retinotopic and higher-level category-selective (i.e., FFA, PPA) areas. Conversely, LIM activity decreased significantly in response to large compared with small visual stimuli. Thus, the LIM response was inverse to both the above psychophysics on salience and to the fMRI responses in classic visual cortex.

A similar conclusion arises from manipulations of retinotopic eccentricity. Psychophysically, objects presented in the periphery are less likely to be detected by observers (Carrasco and Chang 1995; Wolfe et al. 1998). Again these results are inconsistent with our results in LIM, in which extensive manipulation of retinotopic eccentricity did not significantly reduce LIM activity. Such results suggest that LIM may not contribute directly to sensory perception, although it may receive a small input from visual cortex (see Fig. 6 and below).

Self-Referential Processing in LIM

At face value, this hypothesis that LIM does not contribute in sensory perception seems at odds with reports that (at least) parts of STS and adjacent areas are involved in encoding face and body motion (Fig. 5; also see Puce et al. 1998; Haxby et al. 2000; Beauchamp et al. 2003; Thompson et al. 2007; Jastorff and Orban 2009). However, 1 unifying possibility is that LIM is involved in self-referential processes.

Self-referential processes encode different aspects of "self" such as the emotional self, the spatial self, the facial self, and the social self (for review, see Northoff et al. 2006; Buckner et al. 2008). Presumably, neural processes underlying these self-referential functions are recruited when the task and/or stimuli are experienced as related to one's own person (Northoff et al. 2006).

Self-referential processing was initially linked to activity in DMN main hubs (Gusnard et al. 2001; Mitchell et al. 2006; Buckner et al. 2008). However, recent studies (e.g., Pfeifer et al. 2007; Andrews-Hanna et al. 2010) showed that activity within LTC is also stronger during self-referential decision-making, compared with control tasks. Furthermore, this study reported that the same area is more active during metallization of the "present self" rather than "future self". The activation during self-referential tasks might reflect (at least partly) a higher semantic memory

retrieval load during the self-referential compared with the control tasks (Cabeza and Nyberg 2000; Svoboda et al. 2006).

Consistent with this self-referential hypothesis, 1 interpretation of our findings in Experiment 1–4 is that the "self-unrelated" stimuli used here produce varying levels of exogenous attention. That is, our visual stimuli act like distracters, which shift neural and attentional resources away from the self-referential processes and toward sensory perception. According to this idea, the effect in LIM should also vary systematically as a function of the size/number of the visual stimuli—in accord with our results. By extension, it could be argued that the face- and body-motion-selective activity reported in this area (Fig. 5*A*,*B*) arises secondarily from comparing these visual stimuli to self-related (internal) representations. However, further experiments are necessary to test these hypotheses.

Distributed Attention and the Sentinel Hypothesis

Previous studies have suggested that DMN activity is linked to low-level monitoring of the external environment, during which subjects distribute their attention uniformly across the visual field (Ghatan et al. 1995, Shulman et al. 1997; Gusnard et al. 2001; Gilbert et al. 2007; Hahn et al. 2007). According to this "sentinel hypothesis," the main difference between 1) the directed task conditions which decrease activity within DMN and 2) passive conditions which increase DMN activity is a difference in the distribution of attention (i.e., focused vs. distributed) during these 2 conditions.

Although our study was not designed to test different aspects of the sentinel hypothesis, our results (Experiment 4) showed that LIM size sensitivity appeared mainly when subjects distribute their attention throughout the visual field, and it weakened significantly during focused attention. In contrast to LIM, all classic visual areas showed size sensitivity during both central and distributed attention. These results support the sentinel hypothesis, in that the distribution of attention influences activity within LIM (a DMN subarea). However, in contrast to the prediction of the sentinel hypothesis, the results of Experiment 4A and 4B showed that the level of fMRI activity in LIM was higher during focused (rather than distributed) attention. In other words, although our results are consistent with the sentinel hypothesis with regard to the overall importance of attentional state, that hypothesis did not correctly predict the level of LIM activity in different attentional states.

"Suppression" of BOLD Responses in LIM?

Available evidence suggests that BOLD responses reflect both slow (presynaptic) and fast (somatic) electrophysiological components, with a mild bias for the former (Logothetis et al. 2001). Given this, how should we interpret the stimulus-driven BOLD decrease in LIM?

It is conceptually attractive to assume that LIM activity results from a simple, black-box inversion of the size-selective responses evident in visual cortex. However, localizing the possible brain mechanisms that could accomplish such an inversion is complicated. One problem is that if such an inversion were computed within LIM, the presynaptic inputs and the action potentials could potentially drive the BOLD response in opposite directions. For instance, 1) increased firing to larger objects arising in classic visual cortex would presumably increase BOLD responses in any inhibitory presynaptic terminals on visual-recipient neurons located within LIM, whereas 2) resultant axon potentials generated within such LIM neurons could decrease, which could decrease the overall BOLD response.

This quandary can be avoided by assuming that a signal inversion is computed at a prior brain site that is physically remote from (likely posterior to) LIM, within or near classic visual cortex. By this idea, LIM would reflect only the decreased rate of action potentials arriving in LIM, i.e., the presynaptic components would have no competing influence. If confirmed, the size-related BOLD decrease in LIM could in fact reflect a true suppression of electrophysiological activity, which occurs at an immediately prior level.

Another possibility is that the size-inverted response in LIM arises from a less direct, top-down influence from frontal or parietal cortex. That is, input from visual cortex influences activity within higher-level association areas (e.g., the frontoparietal network), thus affecting activity within LIM, via connections between frontoparietal network and LIM.

Functional Connections of LIM

Experiment 6 suggests that different areas of visual cortex have different functional connections with anterior and posterior LIM. Based on the positive (rather than negative) correlation between the resting state activity fluctuation in anterior LIM and multiple areas in middle and higher levels of visual cortex, the reversal of the size function in anterior LIM may reflect local processes within the LIM, rather than a direct suppressive input from the visual areas (see above).

LIM activity may also be influenced by input from the main hubs of DMN (i.e., the PCC and mPFC). This hypothesis is consistent with our functional connection evidence showing that posterior LIM is strongly connected with the DMN main hubs and dorsolateral frontal cortex (Fig. 6). Thus, the inverted size function in LIM may reflect (at least partly) an input from other parts of DMN, which in turn is connected with visual cortex. Of course, the reality might lie somewhere in between, including parts of 1 or more of the above models. For instance, local processes and input from other areas could both contribute to the reversed size function in LIM.

Functional Heterogeneity within LIM

The results of Experiments 1–4 showed a common dependence on stimulus size, number, and attention throughout LIM. On the other hand, results of our functional connectivity measurements (Experiment 6) and our meta-analysis of previous fMRI results (Fig. 5) suggest that LIM spans different functional subregions.

Specifically, a posterior portion of LIM shows 1) a strong "positive" functional connection with the main DMN hubs (i.e., PCC and mPFC), 2) "negative" functional connection to mid-level visual areas, and 3) that region overlaps cortical sites in which fMRI has been related to ToM. Together, these results support the hypothesis that a common neural network is involved in ToM and DMN. In contrast, a more anterior portion of LIM shows 1) a "positive" functional connection with mid and high-level visual areas and 2) overlap with fMRI sites involved in understanding other people's facial and body motion.

LIM in Nonhuman Primates?

Previous comparative studies suggest that humans and monkeys share a similar organization in classic visual cortex (Van Essen et al. 2001; Tootell et al. 2003; Orban et al. 2004). Within visual cortex, that mapping similarity is strongest in the occipitotemporal

areas, becoming progressively weaker in more dorsal and anterior regions.

Here, our data suggest that macaque monkeys do not have a functional homolog of the human LIM. Despite the use of comparable tasks in both species and extensive scans and training, none of the monkeys showed a reversal of the size function in the predicted region of cortex, analogous to what was so obvious in human LIM.

This finding is consistent with previous comparative studies of face processing in humans and monkeys, which did not find a macaque homolog for the face-selective patch that has been reported in human STS (see also Tsao et al. 2003; Rajimehr et al. 2009). In humans, that STS face-selective patch is located within the anterior/ventral portion of LIM (Fig. 5A). Based on a human-to-monkey map projection, the homolog of this area in monkey is expected to be located anteriorly (and dorsally) relative to the monkey MT, within the superior temporal gyrus (i.e., anterior and dorsal to macaque STS). However, based on moving (rather than stationary) stimuli, a recent study proposed instead that a portion of STS fundus was the monkey homolog of this area (Polosecki et al. 2013).

Inverted Size Function Elsewhere in Monkey Brain

Although we did not find a homolog of LIM in macaque monkeys in the predicted cortical site, those experiments consistently revealed a very small patch of size-inverted response near the main (medial STS) face patch in monkeys. Historically, that medial face patch has been presumed to include the homolog of the human FFA, based on its functional properties and its location in the cortical map (Tsao et al. 2003; Rajimehr et al. 2009; Nasr et al. 2011).

Conclusion

In human subjects, activity in a part of STC (i.e., LIM) changed in response to systematic variations in the extent of the stimulated visual field. However, additional lines of evidence suggest that these apparently externally driven responses can only be interpreted accurately by also considering a strong influence of internal, self-related influences. Specifically 1) the responses to variations in visual stimulus extent were inverse in sign, relative to known responses throughout visual cortex; 2) functional connections showed much stronger links to extra-visual regions, as opposed to visual cortex.

By definition, all of LIM showed selectivity to changes in the extent of visual field stimulation. Despite this, LIM could also be parsed into at least 2 subregions, based on manipulations of either sensory (face or biological motion) and internal (ToM) factors. Functional connections in LIM could also be differentiated into subregions. Thus, overall, human LIM appears to offer an opportunity to further study brain processing in sites where internal and external influences meet and interact. More empirically, our findings suggest that future experiments might well consider both these influences, rather than focusing solely on either internal or external influences.

In monkeys, we did not find evidence for an LIM homolog, at least within the expected region of the cortical map, despite much effort to so. This may indicate that internal, self-reflective processes in the macaques are less prominent than in humans. On the other hand, self-reflective processes in macaques may well occur in different brain locations, or be evident in different experiments, compared with those we found in humans (Mantini et al. 2011).

Supplementary Material

Supplementary material can be found at: http://www.cercor.oxfordjournals.org/.

Funding

This study was supported by National Institutes of Health (NIH Grants R01 MH67529 and R01 EY017081) to RBHT, FWO-Vlaanderen (FWO Grants G0A5613N and G043912N) and IUAP7-11 and PF to WV, the Martinos Center for Biomedical Imaging, the NCRR, the MIND Institute, and the NIMH Intramural Research Program. Funding to pay the Open Access publication charges for this article was provided by NIH Grants R01 EY017081 to RBHT.

Notes

Conflict of Interest: None declared.

References

Allison T, Puce A, McCarthy G. 2000. Social perception from visual cues: role of the STS region. Trends Cogn Sci. 4(7):267–278.

Allison T, Puce A, Spencer DD, McCarthy G. 1999. Electrophysiological studies of human face perception. I: Potentials generated in occipitotemporal cortex by face and non-face stimuli. Cereb Cortex. 9(5):415–430.

Andrews-Hanna JR, Reidler JS, Sepulcre J, Poulin R, Buckner RL. 2010. Functional-anatomic fractionation of the brain's default network. Neuron. 65:550–562.

Anticevic A, Repovs G, Shulman GL, Barch DM. 2010. When less is more: TPJ and default network deactivation during encoding predicts working memory performance. Neuroimage. 49(3):2638–2648.

Arzy S, Molnar-Szakacs I, Blanke O. 2008. Self in time: imagined self-location influences neural activity related to mental time travel. J Neurosci. 28(25):6502–6507.

Ashbridge E, Perrett DI, Oram MW, Jellema T. 2000. Effect of image orientation and size on object recognition: Responses of single units in the macaque monkey temporal cortex. Cogn Neuropsychol. 17(13):13–34.

Avidan G, Tanzer M, Hadj-Bouziane F, Liu N, Ungerleider LG, Behrmann M. 2014. Selective dissociation between core and extended regions of the face processing network in congenital prosopagnosia. Cereb Cortex. 24(6):1565–1578.

Bado P, Engel A, Oliveira-Souza R, Bramati IE, Paiva FF, Basilio R, Sato JR, Tovar-Moll F, Moll J. 2013. Functional dissociation of ventral frontal and dorsomedial default mode network components during resting state and emotional autobiographical recall. Hum Brain Mapp. 35(7):3302–3313.

Beauchamp MS, Lee KE, Haxby JV, Martin A. 2003. fMRI responses to video and point-light displays of moving humans and manipulable objects. J Cogn Neurosci. 15:991–1001.

Bell AH, Malecek NJ, Morin EL, Hadj-Bouziane F, Tootell RBH, Ungerleider LG. 2011. Relationship between functional magnetic resonance imaging-identified regions and neuronal category selectivity. J Neurosci. 31(34):12229–12240.

Bidet-Caulet A, Voisin J, Bertrand O, Fonlupt P. 2005. Listening to a walking human activates the temporal biological motion area. NeuroImage. 28:132–139.

Buckner RL, Andrews-Hanna JR, Schacter DL. 2008. The brain's default network: anatomy, function, and relevance to disease. Ann N Y Acad Sci. 1124:1–38.

Cabeza R, Nyberg L. 2000. Neural bases of learning and memory: functional neuroimaging evidence. Curr Opin Neurol. 13 (4):415–421.

Calvert GA, Campbell R. 2003. Reading speech from still and moving faces: the neural substrates of visible speech. J Cogn Neurosci. 15:57–70.

Carrasco M, Chang I. 1995. The interaction of objective and subjective organizations in a localization search task. Percept Psychophys. 57(8):1134–1150.

Carter EJ, Pelphrey KA. 2006. School-aged children exhibit domain-specific responses to biological motion. Social Neurosci. 1:396–411.

Chadick JZ, Gazzaley A. 2011. Differential coupling of visual cortex with default or frontal-parietal network based on goals. Nat Neurosci. 14(7):830–832.

Corbetta M, Kincade JM, Ollinger JM, McAvoy MP, Shulman GL. 2000. Voluntary orienting is dissociated from target detection in human posterior parietal cortex. Nature Neurosci. 3: 292–297.

Costantini M, Galati G, Ferretti A, Caulo M, Tartaro A, Romani GL, Aglioti SM. 2005. Neural systems underlying observation of humanly impossible movements: an fMRI study. Cereb Cortex. 15:1761–1767.

D'Argembeau A, Collette F, Van der Linden M, Laureys S, Del Fiore G, Degueldre C, Luxen A, Salmon E. 2005. Self-referential reflective activity and its relationship with rest: a PET study. Neuroimage. 25(2):616–624.

D'Argembeau A, Stawarczyk D, Majerus S, Collette F, Van der Linden M, Salmon E. 2010. Modulation of medial prefrontal and inferior parietal cortices when thinking about past, present, and future selves. Social Neurosci. 5(2): 187–200.

David N, Aumann C, Santos NS, Bewernick BH, Eickhoff SB, Newen A, Shah NJ, Fink GR, Vogeley K. 2008. Differential involvement of the posterior temporal cortex in mentalizing but not perspective taking. Soc Cogn Affect Neurosci. 3: 279–289.

Denny BT, Kober H, Wager TD, Ochsner KN. 2012. A meta-analysis of functional neuroimaging studies of self-and other judgments reveals a spatial gradient for mentalizing in medial prefrontal cortex. J Cogn Neurosci. 24(8):1742–1752.

Dilks DD, Julian JB, Paunov AM, Kanwisher N. 2013. The occipital place area is causally and selectively involved in scene perception. J Neurosci. 33(4):1331–1336.

Dodell-Feder D, Koster-Hale J, Bedny M, Saxe R. 2011. fMRI item analysis in a theory of mind task. Neuroimage. 55(2):705–712.

Dubeau MC, Iacoboni M, Koski LM, Markovac J, Mazziotta JC. 2001. Topography for body parts motion in the STS region. Social Neuroscience Abstracts. 27.

Engell AD, Haxby JV. 2007. Facial expression and gaze-direction in human superior temporal sulcus. Neuropsychologia. 45(14): 3234–3241.

Epstein RA, Kanwisher N. 1998. A cortical representation of the local visual environment. Nature. 392:598–601.

Ethofer T, Gschwind M, Vuilleumier P. 2011. Processing social aspects of human gaze: a combined fMRI-DTI study. Neuroimage. 55(1):411–419.

Fischl B. 2012. FreeSurfer. Neuroimage. 62(2):774–781.

Fischl B, Sereno MI, Dale AM. 1999. Cortical surface–based analysis II: inflation, flattening, and a surface–based coordinate system. NeuroImage. 9(2):195–207.

Fox CJ, Iaria G, Barton JJ. 2009. Defining the face processing network: optimization of the functional localizer in fMRI. Hum Brain Mapp. 30(5):1637–1651.

Friston KJ, Holmes AP, Price CJ, Buchel C, Worsley KJ. 1999. Multi subject fMRI studies and conjunction analyses. Neuroimage. 10(4):385–396.

Furl N, Garrido L, Dolan RJ, Driver J, Duchaine B. 2011. Fusiform gyrus face selectivity relates to individual differences in facial recognition ability. J Cogn Neurosci. 23(7): 1723–1740.

Gallagher HL, Frith CD. 2003. Functional imaging of 'theory of mind'. Trends Cogn Sci. 7(2):77–83.

Gallagher HL, Happé F, Brunswick N, Fletcher PC, Frith U, Frith CD. 2000. Reading the mind in cartoons and stories: an fMRI study of theory of mind in verbal and nonverbal tasks. Neuropsychologia. 38:1–21.

Gazzola V, Aziz-Zadeh L, Keysers C. 2006. Empathy and the somatotopic auditory mirror system in humans. Curr Biol. 16: 1824–1829.

Gazzola V, Rizzolatti G, Wicker B, Keysers C. 2007. The anthropomorphic brain: the mirror neuron system responds to human and robotic actions. Neuroimage. 35:1674–1684.

Ghatan PH, Hsieh JC, Wirsen-Meurling A, Wredling R, Eriksson L, Stone-Elander S, Levander S, Ingvar M. 1995. Brain activation induced by the perceptual maze test: a PET study of cognitive performance. Neuroimage. 2(2):112–124.

Gilbert SJ, Dumontheil I, Simons JS, Frith CD, Burgess PW. 2007. Comment on "Wandering minds: the default network and stimulus-independent thought". Science. 317:43.

Gobbini MI, Koralek AC, Bryan RE, Montgomery KJ, Haxby JV. 2007. Two takes on the social brain: a comparison of theory of mind tasks. J Cogn Neurosci. 19:1803–1814.

Greene JD, Nystrom LE, Engell AD, Darley JM, Cohen JD. 2004. The neural bases of cognitive conflict and control in moral judgment. Neuron. 44:389–400.

Greene J, Sommerville RB, Nystrom LE, Darley JM, Cohen JD. 2001. An fMRI investigation of emotional engagement in moral judgment. Science. 293:2105–2108.

Greicius MD, Krasnow B, Reiss AL, Menon V. 2003. Functional connectivity in the resting brain: a network analysis of the default mode hypothesis. Proc Natl Acad Sci USA. 100: 253–258.

Greicius MD, Menon V. 2004. Default-mode activity during a passive sensory task: uncoupled from deactivation but impacting activation. J Cogn Neurosci. 16:1484–1492.

Grèzes J, Armony JL, Rowe J, Passingham RE. 2003. Activations related to 'mirror' and 'canonical' neurons in the human brain: an fMRI study. NeuroImage. 18:928–937.

Grosbras MH, Paus T. 2006. Brain networks involved in viewing angry hands and faces. Cereb Cortex. 16:1087–1096.

Grossman ED, Blake R. 2002. Brain areas active during visual perception of biological motion. Neuron. 35:1167–1175.

Grill-Spector K. 2003. The neural basis of object perception. Curr Opin Neurobiol. 13(2):159–166.

Grill-Spector K, Kourtzi Z, Kanwisher N. 2001. The lateral occipital complex and its role in object recognition. Vision Res. 41(10): 1409–1422.

Gusnard DA, Akbudak E, Shulman GL, Raichle ME. 2001. Medial prefrontal cortex and self-referential mental activity: relation to a default mode of brain function. Proc Natl Acad Sci USA. 98:4259:64.

Hagmann P, Cammoun L, Gigandet X, Meuli R, Honey CJ, Wedeen VJ, Sporns O. 2008. Mapping the structural core of human cerebral cortex. PLoS Biol. 6:e159.

Hahn B, Ross TJ, Stein EA. 2007. Cingulate activation increases dynamically with response speed under stimulus unpredictability. Cereb Cortex. 17:1664–1671.

Hamilton AC, Grafton S. 2006. Goal representation in human anterior intraparietal sulcus. J Neurosci. 26:1133–1137.
Haxby JV, Hoffman EA, Gobbini MI. 2000. The distributed human neural system for face perception. Trends Cogn Sci. 4(6): 223–233.
Heatherton TF. 2011. Neuroscience of self and self-regulation. Ann Rev Psychol. 62:363.
Heekeren HR, Wartenburger I, Schmidt H, Prehn K, Schwintowski HP, Villringer A. 2005. Influence of bodily harm on neural correlates of semantic and moral decision-making. NeuroImage. 24:887–897.
Heekeren HR, Wartenburger I, Schmidt H, Schwintowski HP, Villringer A. 2003. An fMRI study of simple ethical decision-making. Neuroreport. 14(9):1215–1219.
Hinds OP, Rajendran N, Polimeni JR, Augustinack JC, Wiggins G, Wald LL, Diana Rosas H, Potthast A, Schwartz EL, Fischl B. 2008. Accurate prediction of V1 location from cortical folds in a surface coordinate system. Neuroimage. 39(4): 1585–1599.
Hooker CI, Paller KA, Gitelman DR, Parrish TB, Mesulam M, Reber PJ. 2003. Brain networks for analyzing eye gaze. Cogn Brain Res. 17(2):406–418.
Hynes CA, Baird AA, Grafton ST. 2006. Differential role of the orbitofrontal lobe in emotional versus cognitive perspective-taking. Neuropsychologia. 44:374–383.
Ishai A, Schmidt CF, Boesiger P. 2005. Face perception is mediated by a distributed cortical network. Brain Res Bull. 67(1):87–93.
Ito M, Tamura H, Fujita I, Tanaka K. 1995. Size and Position Invariance of Neuronal Responses in Monkey Inferoterotemporal Cortex. J Neurophysiol. 73:218–226.
Jastorff J, Orban GA. 2009. Human functional magnetic resonance imaging reveals separation and integration of shape and motion cues in biological motion processing. J Neurosci. 29 (22):7315–7329.
Johansson G. 1973. Visual perception of biological motion and a model for its analysis. Percept Psychophys. 14(2):201–211.
Johnson-Frey SH, Newman-Nordlund R, Grafton ST. 2005. A distributed left hemisphere network active during planning of everyday tool. Cereb Cortex. 6:681–695.
Jolicoeur P. 1987. A size-congruency effect in memory for visual shape. Mem Cogn. 15(6):531–543.
Julian JB, Fedorenko E, Webster J, Kanwisher N. 2012. An algorithmic method for functionally defining regions of interest in the ventral visual pathway. Neuroimage. 60(4): 2357–2364.
Kanwisher N. 2010. Functional specificity in the human brain: a window into the functional architecture of the mind. Proc Natl Acad Sci USA. 107(25):11163–11170.
Kanwisher N, McDermott J, Chun M. 1997. The fusiform face area: a module in human extrastriate cortex specialized for the perception of faces. J Neurosci. 17:4302–4311.
Kobayashi C, Glover GH, Temple E. 2007. Children's and adults' neural bases of verbal and nonverbal 'theory of mind'. Neuropsychologia. 45:1522–1532.
Kojima T, Onoe H, Hikosaka K, Tsutsui KI, Tsukada H, Watanabe M. 2009. Default mode of brain activity demonstrated by positron emission tomography imaging in awake monkeys: higher rest-related than working memory-related activity in medial cortical areas. J Neurosci. 29(46):14463–14471.
Konkle T, Oliva A. 2012. A real-world size organization of object responses in occipito-temporal cortex. Neuron. 74:1114–1124.
Leslie AM, Friedman O, German TP. 2004. Core mechanisms in 'theory of mind. Trends Cogn Sci. 8:528–533.
Liu J, Harris A, Kanwisher N. 2010. Perception of face parts and face configurations: an fMRI study. J Cogn Neurosci. 22 (1):203–211.
Logothetis NK, Pauls J, Augath M, Trinath T, Oeltermann A. 2001. Neurophysiological investigation of the basis of the fMRI signal. Nature. 412(6843):150–157.
Makuuchi M. 2005. Is Broca's area crucial for imitation? Cereb Cortex. 15:563–570.
Malach R, Reppas JB, Benson RR, Kwong KK, Jiang H, Kennedy WA, Ledden PJ, Brady TJ, Tootell RBH. 1995. Object-related activity revealed by functional magnetic resonance imaging in human occipital cortex. Proc Natl Acad Sci USA. 92(18): 8135–8139.
Mantini D, Gerits A, Nelissen K, Durand JB, Joly O, Simone L, Sawamura H, Wardak C, Orban GA, Buckner RL, et al. 2011. Default mode of brain function in monkeys. J Neurosci. 31 (36):12954–12962.
Mantini D, Vanduffel W. 2013. Emerging roles of the brain's default network. Neuroscientist. 19(1):76–87.
Mars RB, Sallet J, Neubert FX, Rushworth MF. 2013. Connectivity profiles reveal the relationship between brain areas for social cognition in human and monkey temporoparietal cortex. Proc Natl Acad Sci USA. 110(26):10806–10811.
Mason MF, Norton MI, Van Horn JD, Wegner DM, Grafton ST, Macrae CN. 2007. Wandering minds: the default network and stimulus-independent thought. Science. 315:393–395.
Mazoyer B, Zago L, Mellet E, Bricogne S, Etard O, Houde O, Crivello F, Joliot M, Petit L, Tzourio-Mazoyer N. 2001. Cortical networks for working memory and executive functions sustain the conscious resting state in man. Brain Res Bull. 54 (3):287–298.
McKiernan KA, D'Angelo BR, Kaufman JN, Binder JR. 2006. Interrupting the "stream of consciousness": an fMRI investigation. Neuroimage. 29:1185–1191.
Mitchell JP. 2008. Activity in right temporo-parietal junction is not selective for theory of mind. Cereb Cortex. 18:262–271.
Mitchell JP, Macrae CN, Banaji MR. 2006. Dissociable medial prefrontal contributions to judgments of similar and dissimilar others. Neuron. 50:655–663.
Moll J, de Oliveira-Souza R, Bramati IE, Grafman J. 2002. Functional networks in emotional moral and nonmoral social judgments. NeuroImage. 16:696–703.
Molnar-Szakacs I, Uddin LQ. 2013. Self-processing and the default mode network: interactions with the mirror neuron system. Front Hum Neurosci. 7:571.
Morris JP, Pelphrey KA, McCarthy G. 2005. Regional brain activation evoked when approaching a virtual human on a virtual walk. J Cogn Neurosci. 17:1744–1752.
Nasr S, Devaney KJ, Tootell RBH. 2013. Spatial encoding and underlying circuitry in scene-selective cortex. Neuroimage. 83:892–900.
Nasr S, Liu N, Devaney KJ, Yue X, Rajimehr R, Ungerleider LG, Tootell RBH. 2011. Scene-selective cortical regions in human and non-human primates. J Neurosci. 31(39):13771–13785.
Nasr S, Tootell RBH. 2012. Role of fusiform and anterior temporal cortical areas in facial recognition. Neuroimage. 63(3): 1743–1753.
Nelissen K, Vanduffel W, Orban GA. 2006. Charting the lower superior temporal region, a new motion-sensitive region in monkey superior temporal sulcus. J Neurosci. 26(22): 5929–5947.
Northoff G, Heinzel A, de Greck M, Bermpohl F, Dobrowolny H, Panksepp J. 2006. Self-referential processing in our brain - a

meta-analysis of imaging studies on the self. Neuroimage. 31 (1):440–457.
Ochsner K, Knierim K, Ludlow D, Hanelin J, Ramachandran T, Glover G, Mackey S. 2004. Reflecting upon feelings: an fMRI study of neural systems supporting the attribution of emotion to self and other. J Cogn Neurosci. 16(10):1746–1772.
Ohnishi T, Moriguchi Y, Matsuda H, Mori T, Hirakata M, Imabayashi E, Hirao K, Nemoto K, Kaga M, Inagaki M, et al. 2004. The neural network for the mirror system and mentalizing in normally developed children: an fMRI study. NeuroReport. 15:1483–1487.
Op De Beeck H, Vogels R. 2000. Spatial sensitivity of macaque inferior temporal neurons. J Compar Neurol. 426(4):505–518.
Orban GA, Van Essen D, Vanduffel W. 2004. Comparative mapping of higher visual areas in monkeys and humans. Trends Cogn Sci. 8:315–324.
Peelen MV, Wiggett AJ, Downing PE. 2006. Patterns of fMRI activity dissociate overlapping functional brain areas that respond to biological motion. Neuron. 49:815–822.
Pelphrey KA, Morris JP, Michelich CR, Allison T, McCarthy G. 2005. Functional anatomy of biological motion perception in posterior temporal cortex: an fMRI study of eye, mouth and hand movements. Cereb Cortex. 15:1866–1876.
Perner J, Aichhorn M, Kronbichler M, Staffen W, Ladurner G. 2006. Thinking of mental and other representations: the roles of left and right temporo-parietal junction. J Neurosci. 1:245–258.
Peuskens H, Vanrie J, Verfaillie K, Orban GA. 2005. Specificity of regions processing biological motion. Eur J Neurosci. 21: 2864–2875.
Pfeifer J, Lieberman M, Dapretto M. 2007. "I know you are but what am I?!": neural bases of self-and social knowledge retrieval in children and adults. J Cogn Neurosci. 19(8): 1323–1337.
Pierno AC, Becchio C, Wall MB, Smith AT, Castiello U. 2006. Transfer of interfered motor patterns to self from others. Eur J Neurosci. 23:1949–1955.
Pinsk MA, Arcaro M, Weiner KS, Kalkus JF, Inati SJ, Gross CG, Kastner S. 2009. Neural representations of faces and body parts in macaque and human cortex: a comparative FMRI study. J Neurophysiol. 101(5):2581–2600.
Prehn K, Wartenburger I, Mériau K, Scheibe C, Goodenough OR, Villringer A, van der Meer E, Heekeren HR. 2008. Individual differences in moral judgment competence influence neural correlates of socio-normative judgments. Soc Cogn Affect Neurosci. 3:33–46.
Polosecki P, Moeller S, Schweers N, Romanski LM, Tsao DY, Freiwald WA. 2013. Faces in motion: selectivity of macaque and human face processing areas for dynamic stimuli. J Neurosci. 33(29):11768–11773.
Popivanov ID, Jastorff J, Vanduffel W, Vogels R. 2012. Stimulus representations in body-selective regions of the macaque cortex assessed with event-related fMRI. NeuroImage. 63(2): 723–741.
Puce A, Allison T, Asgari M, Gore JC, McCarthy G. 1996. Differential sensitivity of human visual cortex to faces, letterstrings, and textures: a functional magnetic resonance imaging study. J Neurosci. 16(16):5205–5215.
Puce A, Allison T, Bentin S, Gore JC, McCarthy G. 1998. Temporal cortex activation in humans viewing eye and mouth movements. J Neurosci. 18(6):2188–2199.
Qin P, Northoff G. 2011. How is our self related to midline regions and the default-mode network? Neuroimage. 57 (3):1221–1233.
Raichle ME, MacLeod AM, Snyder AZ, Powers WJ, Gusnard DA, Shulman GL. 2001. A default mode of brain function. Proc Natl Acad Sci USA. 98:676–682.
Rajimehr R, Young JC, Tootell RBH. 2009. An anterior temporal face patch in human cortex, predicted by macaque maps. Proc Natl Acad Sci USA. 106(6):1995–2000.
Ramnani N, Miall RC. 2004. A system in the human brain for predicting the actions of others. Nat Neurosci. 7:85–90.
Rilling JK, Barks SK, Parr LA, Preuss TM, Faber TL, Pagnoni G, Brmner JD, Votaw JR. 2007. A comparison of resting-state brain activity in humans and chimpanzees. Proc Natl Acad Sci USA. 104(43):17146–17151.
Robertson D, Snarey J, Ousley O, Keith-Harenski K, Bowmand FD, Gilkey R, Kilts C. 2007. The neural processing of moral sensitivity to issues of justice and care. Neuropsychologia. 45:755–766.
Said CP, Haxby JV, Todorov A. 2011. Brain systems for assessing the affective value of faces. Philos Trans R Soc B Biol Sci. 366 (1571):1660–1670.
Sakreida K, Schubotz RI, Wolfensteller U, Cramon DY. 2005. Motion clasdependency in observer' motor areas revealed by functional magnetic resonance imaging. J Neurosci. 25:1335–1342.
Santi A, Servos P, Vatikiotis-Bateson E, Kuratate T, Munhall K. 2003. Perceiving biological motion: dissociating visible speech from walking. J Cogn Neurosci. 15:800–809.
Saxe R, Kanwisher N. 2003. People thinking about people - the role of the temporo-parietal junction in theory of mind. NeuroImage. 19:1835–1842.
Saxe R, Powell L. 2006. It's the thought that counts: specific brain regions for one component of theory of mind. Psychol Sci. 17 (8):692–699.
Saxe R, Xiao DK, Kovacsc G, Perrett DI, Kanwisher N. 2004. A region of right posterior superior temporal sulcus responds to observed intentional actions. Neuropsychologia. 42:1435–1446.
Saygin AP, Wilson SM, Hagler DJ, Bates E, Sereno MI. 2004. Point-light biological motion perception activates human premotor cortex. J Neurosci. 24(27):6181–6188.
Schacter DL, Addis DR. 2007. The cognitive neuroscience of constructive memory: remembering the past and imagining the future. Philos Trans R Soc B Biol Sci. 362(1481): 773–786.
Schnell K, Heekeren K, Schnitker R, Daumann J, Weber J, Heszelmann V, Moller-Hartmann W, Thron A, Gouzoulis-Mayfrank E. 2007. An fMRI approach to particularize the frontoparietal network for visuomotor action monitoring: detection of incongruence between test subjects' actions and resulting perceptions. NeuroImage. 34:332–341.
Schubotz RI, von Cramon DY. 2004. Sequences of abstract nonbiological stimuli share ventral premotor cortex with action observation and imagery. J Neurosci. 24:5467–5474.
Schultz J, Brockhaus M, Bülthoff HH, Pilz KS. 2013. What the human brain likes about facial motion. Cerebral Cortex. 23 (5):1167–1178.
Sebastian CL, Fontaine NM, Bird G, Blakemore SJ, De Brito SA, McCrory EJ, Viding E. 2011. Neural processing associated with cognitive and affective Theory of Mind in adolescents and adults. Soc Cogn Affect Neurosci. doi:10.1093/scan/nsr023.
Sereno MI, Tootell RBH. 2005. From monkeys to humans: what do we now know about brain homologies? Curr Opin Neurobiol. 15:135–144.
Shulman GL, Astafiev SV, McAvoy MP, d'Avossa G, Corbetta M. 2007. Right TPJ deactivation during visual search: functional significance and support for a filter hypothesis. Cereb Cortex. 17(11):2625–2633.

Shulman GL, Fiez JA, Corbetta M, Buckner RL, Miezin FM, Raichle ME, Petersen SE. 1997. Common blood flow changes across visual tasks. 2. Decreases in cerebral cortex. J Cogn Neurosci. 9:648–663.

Sommer M, Döhnel K, Sodian B, Meinhardt J, Thoermer C, Hajak G. 2007. Neural correlates of true and false belief reasoning. NeuroImage. 35:1378–1384.

Spreng RN, Grady CL. 2010. Patterns of brain activity supporting autobiographical memory, prospection, and theory of mind, and their relationship to the default mode network. J Cogn Neurosci. 22(6):1112–1123.

Spreng RN, Mar RA, Kim AS. 2009. The common neural basis of autobiographical memory, prospection, navigation, theory of mind, and the default mode: a quantitative meta-analysis. J Cogn Neurosci. 21(3):489–510.

Svoboda E, McKinnon MC, Levine B. 2006. The functional neuroanatomy of autobiographical memory: a meta-analysis. Neuropsychologia. 44:2189–2208.

Thompson JC, Hardee JE, Panayiotou A, Crewther D, Puce A. 2007. Common and distinct brain activation to viewing dynamic sequences of face and hand movements. Neuroimage. 37 (3):966–973.

Tootell RBH, Hadjikhani N, Hall EK, Marrett S, Vanduffel W, Vaughan JT, Dale AM. 1998. The retinotopy of visual spatial attention. Neuron. 21(6):1409–1422.

Tootell RBH, Tsao D, Vanduffel W. 2003. Neuroimaging weighs in: humans meet macaques in "primate" visual cortex. J Neurosci. 23(10):3981–3989.

Tsao DY, Freiwald WA, Knutsen TA, Mandeville JB, Tootell RBH. 2003. The representation of faces and objects in Macaque Cerebral Cortex. Nat Neurosci. 6:989–995.

Vaina LM, Solomon J, Chowdhury S, Sinha P, Belliveau JW. 2001. Functional neuroanatomy of biological motion perception in humans. Proc Natl Acad Sci USA. 98:11656–11661.

van der Meer L, Costafreda S, Aleman A, David AS. 2010. Self-reflection and the brain: a theoretical review and meta-analysis of neuroimaging studies with implications for schizophrenia. Neurosci Biobehav Rev. 34(6):935–946.

Villarreal M, Fridman EA, Amengual A, Falasco G, Gerscovich ER, Ulloa ER, Leiguarda RC. 2008. The neural substrate of gesture recognition. Neuropsychologia. 46:2371–2382.

Vanduffel W, Fize D, Mandeville JB, Nelissen K, Hecke PV, Tootell RBH, Orban GA. 2001. Visual motion processing investigated using contrast agent-enhanced fMRI in awake behaving monkeys. Neuron. 32(4):565–577.

Van Essen DC. 2005. A population-average, landmark- and surface-based (PALS) atlas of human cerebral cortex. Neuroimage. 28:635–662.

Van Essen DC, Lewis JW, Drury HA, Hadjikhani N, Tootell RBH, Bakircioglu M, Miller MI. 2001. Mapping visual cortex in monkeys and humans using surface-based atlases. Vision Res. 41:1359–1378.

Van Overwalle F, Baetens K. 2009. Understanding others' actions and goals by mirror and mentalizing systems: a meta-analysis. Neuroimage. 48(3):564–584.

Vincent JL, Patel GH, Fox MD, Snyder AZ, Baker JT, Van Essen DC, Zempel JM, Snyder LH, Corbetta M, Raichle ME. 2007. Intrinsic functional architecture in the anaesthetized monkey brain. Nature. 447(7140):83–86.

Wheaton KJ, Thompson JC, Syngeniotis A, Abbott DF, Puce A. 2004. Viewing the motion of human body parts activates different regions of premotor, temporal, and parietal cortex. NeuroImage. 22:277–288.

Wicker B, Ruby P, Royet JP, Fonlupt P. 2003. A relation between rest and the self in the brain? Brain Res Rev. 43(2):224–230.

Winston JS, Henson RNA, Fine-Goulden MR, Dolan RJ. 2004. fMRI-adaptation reveals dissociable neural representations of identity and expression in face perception. J Neurophysio. 92(3):1830–1839.

Wolfe JM, O'Neill P, Bennett SC. 1998. Why are there eccentricity effects in visual search? Visual and attentional hypotheses. Percept Psychophys. 60(1):140–156.

Yeo BT, Krienen FM, Sepulcre J, Sabuncu MR, Lashkari D, Hollinshead M, Roffman JL, Smoller JW, Zollei L, Polimeni JR, et al. 2011. The organization of the human cerebral cortex estimated by intrinsic functional connectivity. J Neurophysiol. 106(3):1125–1165.

Young L, Cushman F, Hauser M, Saxe R. 2007. The neural basis of the interaction between theory of mind and moral judgment. Proc Natl Acad Sci USA. 104:8235–8240.

Young L, Dodell-Feder D, Saxe R. 2010. What gets the attention of the temporo-parietal junction? An fMRI investigation of attention and theory of mind. Neuropsychologia. 48(9): 2658–2664.

Young L, Saxe R. 2008. The neural basis of belief encoding and integration in moral judgment. NeuroImage. 40:1912–1920.